Nucleic Acids Research, 2024, **52**, 7825–7842
https://doi.org/10.1093/nar/gkae486
Advance access publication date: 13 June 2024
Nucleic Acid Enzymes

Eukaryotic AlaX provides multiple checkpoints for quality and quantity of aminoacyl-tRNAs in translation

Zi-Han Li[1] and Xiao-Long Zhou[1,2,*]

[1]Key Laboratory of RNA Innovation, Science and Engineering, CAS Center for Excellence in Molecular Cell Science, Shanghai Institute of Biochemistry and Cell Biology, Chinese Academy of Sciences, University of Chinese Academy of Sciences, 320 Yue Yang Road, Shanghai 200031, China
[2]Key Laboratory of Systems Health Science of Zhejiang Province, School of Life Science, Hangzhou Institute for Advanced Study, University of Chinese Academy of Sciences, Hangzhou 310024, China

*To whom correspondence should be addressed. Tel: +86 21 5492 1247; Fax: +86 21 5492 1011; Email: xlzhou@sibcb.ac.cn

Abstract

Translational fidelity relies critically on correct aminoacyl-tRNA supply. The *trans*-editing factor AlaX predominantly hydrolyzes Ser-tRNA^{Ala}, functioning as a third sieve of alanyl-tRNA synthetase (AlaRS). Despite extensive studies in bacteria and archaea, the mechanism of *trans*-editing in mammals remains largely unknown. Here, we show that human AlaX (hAlaX), which is exclusively distributed in the cytoplasm, is an active *trans*-editing factor with strict Ser-specificity. *In vitro*, both hAlaX and yeast AlaX (*Sc*AlaX) were capable of hydrolyzing nearly all Ser-mischarged cytoplasmic and mitochondrial tRNAs; and robustly edited cognate Ser-charged cytoplasmic and mitochondrial tRNA^{Ser}s. *In vivo* or cell-based studies revealed that loss of *Sc*AlaX or hAlaX readily induced Ala- and Thr-to-Ser misincorporation. Overexpression of hAlaX impeded the decoding efficiency of consecutive Ser codons, implying its regulatory role in Ser codon decoding. Remarkably, yeast cells with *Sc*AlaX deletion responded differently to translation inhibitor treatment, with a gain in geneticin resistance, but sensitivity to cycloheximide, both of which were rescued by editing-capable *Sc*AlaX, alanyl- or threonyl-tRNA synthetase. Altogether, our results demonstrated the previously undescribed editing peculiarities of eukaryotic AlaXs, which provide multiple checkpoints to maintain the speed and fidelity of genetic decoding.

Graphical abstract

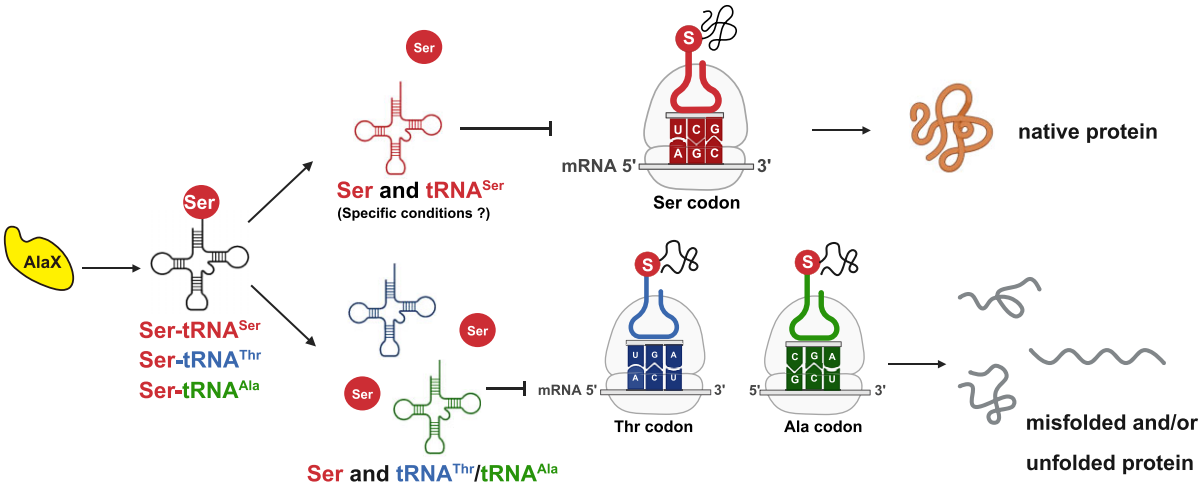

Introduction

Accurate decoding of genetic code is critical for all organisms. Mistranslation occurs when an amino acid is ligated with an incorrect tRNA and is subsequently misincorporated into a nascent protein (1,2).

Aminoacyl-tRNA synthetases (aaRSs) (2), ubiquitously expressed housekeeping genes in all domains of life, play a pivotal role in ensuring high accuracy in protein synthesis. AaRSs charge tRNAs with their cognate amino acids to generate aminoacyl-tRNAs (aminoacylation) in a two-step reaction (3,4). An amino acid is first activated by adenosine triphosphate (ATP) to form an aminoacyl-adenylate (aa-AMP) intermediate, followed by the transfer of the aminoacyl moiety from aa-AMP to A76 of tRNAs. During aminoacylation, the active site of a given aaRS functions as a coarse sieve (the first sieve) that excludes most amino acids with larger sizes; however, some non-cognate amino acids with similar sizes and/or chemical structures are misactivated and then misligated with

Received: January 30, 2024. **Editorial Decision:** May 21, 2024. **Accepted:** May 27, 2024

tRNAs (5). The resulting mischarged tRNAs (such as Ser-tRNA^{Thr} and Ser-tRNA^{Ala}), if not cleared, can potentially lead to amino acid misincorporation during translation (1). To overcome this limitation and ensure the fidelity of protein synthesis, approximately half of the existing aaRSs have evolved a proofreading (editing) function to remove mischarged tRNAs (1,6). The editing reaction is usually performed by a separate editing domain, appended or inserted later in evolution, which functions as the second fine sieve, targeting only misactivated non-cognate amino acids (7,8). In the past few decades, numerous studies have underscored that the editing activity of aaRSs (*cis*-editing) is one of the most critical mechanisms for high accuracy of protein synthesis, the impairment of which causes profound deleterious effects on cell homeostasis in the three domains of life and leads to various mammalian diseases, including severe neuropathologies and cardioproteinopathies (9–12).

The double-sieve mechanism seems to be insufficient to ensure a high level of accuracy in protein synthesis, as evidenced by the widespread presence of freestanding *trans*-editing factors in all domains of life (2,6). These standalone proteins, including D-aminoacyl-tRNA deacylase (DTD), YbaK, ProX, AlaX, ThrRS-ed and CtdA, display an obvious homology with the *cis*-editing domains in relevant aaRSs (2,6,13–15). The retention of these *trans*-editing factors provides an additional checkpoint for the clearance of mischarged tRNAs, which escape the editing activity of the corresponding aaRSs, and represent the third sieve in tRNA aminoacylation (16).

Alanyl-tRNA synthetase (AlaRS) is the most evolutionarily conserved aaRS. It contains aminoacylation domain (AD), editing domain (ED), and C-terminal domain (C-Ala) (17,18). The ED domain of AlaRS is homologous to that of threonyl-tRNA synthetase (ThrRS), both of which contain a conserved Zinc-binding motif HXXXH or CXXXH. All AlaRSs are inherently unable to distinguish between non-cognate Gly and Ser (19). The generated Gly- or Ser-tRNA^{Ala} is first removed by the ED domain of AlaRS, which is inactive to hydrolyze Ser-tRNA^{Thr}, a substrate of the ED domain of ThrRS, because of its reliance on tRNA^{Ala}-specific G3-U70 recognition during editing (17). However, Ala-to-Ser mistranslation is an ancient problem and a paradox throughout evolution. Even a two-fold reduction in AlaRS editing results in the accumulation of misfolded proteins in Purkinje cells and neurodegeneration in mice (10). Thus, it is reasonable that despite the limited distribution of YbaK in bacteria (20,21), ThrRS-ed in Crenarchaea (22), AlaX, the homology of ED domains of both AlaRS and ThrRS, is conserved in three domains of life to ensure stringent exclusion of Ala-to-Ser mistranslation (16,23).

There are three subfamilies of AlaX based on amino acid sequence and length, including AlaX-S, AlaX-M, and AlaX-L, which contain the Zinc-binding motif. AlaX-L displays homology with ED and C-Ala, whereas AlaX-M corresponds only to the ED of AlaRS. AlaX-S is a minimal AlaX that contains only a fragment of the AlaRS-ED domain (24). To date, most studies on AlaX have been performed using either bacterial or archaeal AlaX (23–26) and, AlaX is widely recognized as a *trans*-editing factor for AlaRS, as all the investigated AlaXs are readily able to hydrolyze Ser-tRNA^{Ala}. Several studies have revealed multiple editing substrates for various AlaXs. For example, *Pyrococcus horikoshii* (*Ph*) AlaX-S is unable to hydrolyze Gly- and Ala-tRNA^{Ala} but clears Ser-tRNA^{Ala} and Ser-tRNA^{Thr} efficiently (23,26). Hydrolysis of Gly-tRNA^{Ala} is carried out by *Ph*AlaX-M (24). *M. barkeri* and *S. solfataricus* AlaXs hydrolyze Gly-tRNA^{Ala} and are inactive in removing Ser-tRNA^{Thr}, Ala-tRNA^{Ala}, and Ser-tRNA^{Ser} (27). Similarly, *Escherichia coli* AlaRS containing only the ED-C-Ala domains fails to remove Ser-tRNA^{Thr} (17). Thus, the precise substrates of AlaXs are ambiguous, and the presence of additional editing substrate(s) in AlaX remains unclear. To date, only few studies have investigated the *in vitro* hydrolytic activity of eukaryotic AlaXs (17,27,28). One study showed that *Saccharomyces cerevisiae* AlaX (*Sc*AlaX) does not hydrolyze Gly- and Ser-tRNA^{Ala}, suggesting that yeast AlaX is no longer an active *trans*-editing factor (27). However, other studies have shown that yeast or mouse AlaX is active in hydrolyzing Ser-tRNA^{Ala} but activity of the latter is regulated by an N-terminal-fused protein (17,19,28). Thus, our understanding of the activity, potential substrate(s), and tRNA recognition mechanisms of eukaryotic AlaX remains limited. Moreover, the cellular distribution of eukaryotic AlaX in the cytoplasm, nucleus, and mitochondria remains unclear. Finally, the cellular functions of eukaryotic AlaX remain largely unknown. The mechanism and role of *trans*-editing in eukaryotic cells require further detailed investigation.

In this study, we systematically investigated human AlaX (hAlaX) encoded by alanyl-tRNA synthetase domain containing 1 (*AARSD1*) and found that it is exclusively distributed in the cytoplasm. We found that both human and yeast AlaXs are active *trans*-editing factors. hAlaX exhibited stringent Ser specificity but displayed editing activity for nearly all naturally generated Ser-charged tRNAs in cells, including Ser-tRNA^{Ala}, Ser-tRNA^{Thr}, Ser-tRNA^{Ser} and Ser-tRNA^{Sec} *in vitro*. Recognition of tRNA by hAlaX was neither L-shape dependent nor specific to the acceptor stem. Widespread editing has also been observed with *Sc*AlaX *in vitro*. Notably, loss of *Sc*AlaX and hAlaX induced Ala-to-Ser and Thr-to-Ser replacements *in vivo* and conferred vulnerability or advantage to yeast cells under different translation elongation inhibition conditions, which are restored by editing-capable AlaRS or ThrRS. In summary, our results suggest that eukaryotic AlaX functions as an unprecedented multi-layer *trans*-editing factor for AlaRS, ThrRS (via Ser-tRNA^{Ala} and Ser-tRNA^{Thr} hydrolysis), and seryl-tRNA synthetase (SerRS) (via Ser-tRNA^{Ser} hydrolysis) to maintain speed and fidelity of messenger RNA (mRNA) translation.

Materials and methods

Materials

Dithiothreitol (DTT), nucleoside triphosphates (NTPs), Tris–HCl, $MgCl_2$, NaCl, KCl, β-mercaptoethanol (β-ME), phenyl methylsulfonyl fluoride (PMSF), isopropyl β- D -1-thiogalactopyranoside (IPTG), and ethylene diamine tetraacetic acid (EDTA) were purchased from Sangon (Shanghai, China). Serine (S4311), Glycine (G2879), Threonine (T8441), Alanine (A7469) were obtained from Sigma-Aldrich (St. Louis, MO, USA). The KOD-Plus Mutagenesis and KOD-Plus-Neo Kits were purchased from TOYOBO (Osaka, Japan). Seamless Cloning Kit, T4 DNA ligase, Lipofectamine 8000, 4′,6-diamidino-2-phenylindole (DAPI) were purchased from Beyotime (Shanghai, China). The Ni^{2+}-NTA Superflow resin was purchased from Qiagen Inc. (Hilden, Germany). [α-^{32}P]ATP (BLU503H) was obtained from Perkin Elmer Inc. (Waltham, MA, USA). Protein standard markers, restriction endonucleases, T4 polynucleotide kinase, Dynabeads Protein

G, MitoTracker, and Alexa Fluor 488-conjugated secondary antibodies were purchased from Thermo Fisher Scientific (Waltham, MA, USA). PrimeScript reverse transcription Master Mix, TALON metal affinity resin, and Yeastmaker Yeast Transformation System 2 were obtained from TaKaRa (Japan). The TRIzol Reagent, deoxyribonucleic acid (DNA) fragment rapid purification kit, and plasmid extraction kit were obtained from Tiangen (Beijing, China). Primer synthesis and DNA sequencing were performed using Biosune or Tsingke (Shanghai, China) kits.

Antibodies

Recombinant hAlaX purified from *E. coli* was used as an antigen to generate an anti-hAlaX antibody (Abclonal, China). Anti-Myc (06549), anti-FLAG (F1804), horseradish peroxidase-labeled anti-mouse, and anti-rabbit secondary antibodies were obtained from Sigma-Aldrich (St. Louis, MO, USA). Anti-His_6 (66005-1-Ig), anti-glyceraldehyde-3-phosphate dehydrogenase (GAPDH) (60004-1-Ig), anti-TOMM40 (18409-1-AP), and anti-Lamin A/C (10298-1-AP) antibodies were purchased from Proteintech (Rosemont, IL, USA). Anti-tubulin (M20005M) antibody was purchased from Abmart (Shanghai, China).

Plasmid construction

The genes encoding hAlaX (UniProt No. Q9BTE6), hAlaRS (UniPort No. P49588), and hDTD1 (UniPort No. Q8TEA8) were amplified from cDNA obtained by reverse transcription of total RNA from human HEK293T cells. The genes encoding *Sc*AlaX (UniProt No. P53960) and *Sc*AlaRS (Uniport No. P40825) were amplified from the BY4741 genome. For gene expression analysis in HEK293T cells, hAlaX gene was inserted between the BamHI and XhoI sites of pCMV-3Tag-3A, pCMV-3Tag-4A or pEGFP-N2. EGFP was amplified from pEGFP-N2 and inserted between the BamHI and XhoI sites into pCMV-3Tag-3A. For gene expression in *E. coli*, hAlaX gene was inserted between the BamHI and XhoI sites of pET28a; hAlaRS gene was inserted between the NdeI and NotI sites of pET30a; hDTD1 gene was inserted between the BamHI and XhoI sites of pET30a; *Sc*AlaX gene was inserted between the BamHI and SalI sites of pRSFDuet1. For gene expression in *S. cerevisiae*, *Sc*AlaRS gene was inserted into p425TEF-C-His_6 (with a C-terminal in-frame DNA sequence encoding a His_6-tag for western blotting) using a Seamless Cloning Kit. Constructs expressing *Sc*ThrRS, *Sc*ThrRS-H151A/H155A, mThrRS-H154A/H158, *Ec*AlaRS-C666A, human cytoplasmic SerRS (hSerRS), mtAlaRS-R663E and mtThrRS-H133A/H137A have been reported previously (12,29–32). Gene mutagenesis was performed according to the procedures provided with the KOD Plus Mutagenesis Kit. The primers used are listed in Supplementary Table S1.

Protein purification

Genes encoding hAlaX and its mutants (hAlaX-C209A, -G377L, -K380A), *Sc*AlaX and its mutant (*Sc*AlaX-C240A) were expressed in *Escherichia coli* BL21 (DE3) cells and induced with 200 μM IPTG when the absorbance at 600 nm (A_{600}) of cell culture reached 0.6, and transformants were cultured overnight at 18°C. Protein purification of *E. coli* transformants was performed using the procedure described in a previous report (33). Proteins were concentrated in storage buffer (50 mM Tris–HCl, pH 8.0 and 150 mM NaCl) and mixed with an equal volume of glycerol. The protein concentration was determined using a Protein Quantification Kit (BCA Assay, Beyotime, Shanghai, China) according to the manufacturer's instructions.

tRNA gene cloning and transcription

Genes encoding human cytoplasmic (hc) $tRNA^{Thr}$(AGU), $tRNA^{Ser}$(GCU and AGA), $tRNA^{Ala}$ and $tRNA^{Sec}$ were incorporated into the pTrc99b plasmid with the T7 promoter at the N-terminus. tRNA transcripts were obtained by *in vitro* T7 RNA polymerase transcription as described previously (34,35).

^{32}P-labeling of tRNA

^{32}P-labeling of tRNAs was performed at 37°C in a mixture containing 60 mM Tris–HCl (pH 8.0), 12 mM $MgCl_2$, 15 μM tRNA, 0.5 mM DTT, 15 μM [^{32}P]ATP, and 10 μM *E. coli* CCA-adding enzyme (CCase) for 5 min (36). Further, 0.8 U/μl pyrophosphatase was added to the mixture and incubated for 2 min. Obtained [^{32}P]tRNA was extracted with Tris-Saturated Phenol (pH 7.7–8.1) and phenol/chloroform/isoamyl alcohol, 12 000 × *g* for 5 min. The aqueous phase was precipitated with ethanol overnight at –20°C, and dissolved in 5 mM $MgCl_2$, as described previously (36).

Preparation of (mis)charged tRNAs

All tRNAs used in this study were either human cytoplasmic or mitochondrial tRNAs. According to a previously described procedure (32), Ala/Ser/Thr/Gly-[^{32}P]$tRNA^{Ala}$ was obtained at 37°C in a reaction mixture (50 μl) containing 50 mM Tris–HCl (pH 7.5), 10 mM $MgCl_2$, 20 mM KCl, 2 mM DTT, 4 mM ATP, 200 mM Ser/Gly/Thr or 1 mM Ala, and 2 μM *Ec*AlaRS-C666A with 10 μM $tRNA^{Ala}$ and [^{32}P]$tRNA^{Ala}$ (1 000 000 CPM). Ser-[^{32}P]$tRNA^{Ser}$, Ser-[^{32}P]$tRNA^{Ser}$ mutants and Ser-[^{32}P]$tRNA^{Sec}$ were prepared at 37°C in a reaction mixture (50 μl) containing 50 mM Tris–HCl (pH 7.5), 10 mM $MgCl_2$, 20 mM KCl, 2 mM DTT, 4 mM ATP, 1 mM Ser and 2 μM SerRS with 10 μM $tRNA^{Ser}$ or $tRNA^{Sec}$ and [^{32}P]$tRNA^{Ser}$, [^{32}P]$tRNA^{Ser}$ mutants or $tRNA^{Sec}$ (1 000 000 CPM). Ser/Thr-[^{32}P]$tRNA^{Thr}$ was prepared at 37°C in a reaction mixture (50 μl) containing 50 mM Tris–HCl (pH 7.5), 10 mM $MgCl_2$, 20 mM KCl, 2 mM DTT, 4 mM ATP, 200 mM Ser or 2 mM Thr, and 2 μM mThrRS-H154A/H158A with 10 μM $tRNA^{Thr}$ and [^{32}P]$tRNA^{Thr}$ (1 000 000 CPM). Ser-[^{32}P]$mtRNA^{Ala}$ and its mutant were obtained at 37°C in a reaction mixture (50 μl) containing 50 mM Tris–HCl (pH 8.0), 20 mM KCl, 10 mM $MgCl_2$, 2 mM DTT, 4 mM ATP, 200 mM Ser and 2 μM mtAlaRS-R663E with 10 μM $mtRNA^{Ala}$ and [^{32}P]$mtRNA^{Ala}$ (1 000 000 CPM). Ser-[^{32}P]$mtRNA^{Ser}$(AGY) was generated at 37°C in a reaction mixture (50 μl) containing 60 mM Tris–HCl (pH 7.5), 15 mM $MgCl_2$, 60 mM KCl, 2 mM DTT, 4 mM ATP, 1 mM Ser and 2 μM mtSerRS with 10 μM $mtRNA^{Ser}$(AGY) and [^{32}P]$mtRNA^{Ser}$(AGY) (1 000 000 CPM). Ser-[^{32}P]$mtRNA^{Thr}$ was prepared at 37°C in a reaction mixture (50 μl) containing 60 mM Tris–HCl (pH 7.5), 10 mM $MgCl_2$, 200 mM Ser and 2 μM mtThrRS-H133A/H137A with 10 μM $mtRNA^{Thr}$ and $mtRNA^{Thr}$ (1 000 000 CPM). The obtained aa-[^{32}P]tRNA was extracted using Tris-Saturated Phenol (pH 4.5) and phenol/chloroform/isoamyl alcohol at 12 000 × *g* for 5 min. The aqueous phase was precipitated with ethanol overnight at –20°C, centrifuged 10 000 × *g* at

4°C for 30 min and dissolved in 5 mM $MgCl_2$, as described previously (36).

Editing assay

The editing assay was carried out at 37°C in a 50 μl reaction mixture containing 50 mM Tris–HCl (pH 6.8), 5 mM $MgCl_2$, 5 mM KCl, 2 mM DTT, 36 000 CPM aa-[^{32}P]tRNA, and 1 μM AlaX or its variant or 1 μM hDTD1. 9 μl samples were placed into ethanol for precipitation with NaAc (pH 5.2) at indicated time intervals. Samples were precipitated in –20°C overnight and centrifuged 10 000 × *g* at 4°C for 30 min. The obtained samples were digested in a 6 μl reaction mixture containing 25 U nuclease S1 for 2 h at 37°C (12). Nuclease S1-generated aa-[^{32}P]AMP (reflecting aa-[^{32}P]tRNA) and [^{32}P]AMP (reflecting free [^{32}P]tRNA) were separated by thin-layer chromatography (TLC). Digestion samples (1.5 μl) of the reaction mixture were loaded on the TLC plates. Separation of aa-[^{32}P]AMP and [^{32}P]AMP was performed in 0.1 M NH_4Ac and 5% acetic acid. The plates were visualized by phosphor imaging, and the data were analyzed using Multi Gauge Version 3.0 software (FUJIFILM) (29). The total amount of (mis)charged tRNAs at each time point was normalized to the initial input of (mis)charged tRNAs at 0 min in the control assays. The amount of (mis)charged tRNAs at each time point was determined as aa-[^{32}P]AMP/([^{32}P]AMP + aa-[^{32}P]AMP).

Cell culture, transfection and Co-IP

HEK293T cells were cultured in Dulbecco's modified Eagle's medium supplemented with 10% fetal bovine serum in a 37°C incubator with 5% CO_2 at a confluence of 70% before transfection with Lipofectamine 8000 transfection reagent according to the manufacturer's protocol. At 24 h after transfection, cells were harvested, washed with ice-cold phosphate-buffered saline (PBS) thrice, and lysed with 1 ml of ice-cold lysis buffer (50 mM Tris–HCl, pH 7.5, 150 mM NaCl, 5 mM ethylenediaminetetraacetic acid, 1% Triton X-100) supplemented with a protease inhibitor cocktail for 15 min at 4°C with rotation. The lysate was centrifuged at 12 000 × *g* for 10 min to remove the debris. The supernatant was incubated with the relevant magnetic beads overnight and then washed thrice with phosphate-buffered saline (PBS) with Tween® detergent (PBST). After adding the twice volume of SDS loading to the beads, samples were boiled at 95°C for 10 min. Co-immunoprecipitation was performed as described previously (37).

Western blotting

Protein samples were separated on a 10% gel in SDS running buffer and transferred onto a methanol-activated polyvinylidene fluoride membrane. The transformed membranes were blocked with 5% milk in PBST for 1 h at room temperature. Immunoblotting was performed using the relevant primary antibody at 4°C overnight, followed by incubation with secondary antibodies, and imaged with an Amersham imager 680 system (GE, CA, USA) as described previously (38).

Immunofluorescence and fluorescence

HEK293T cells were transfected with the specific plasmids. After 24 h, cells were stained with MitoTracker for 30 min and fixed in 4% paraformaldehyde in PBS for 30 min at room temperature. The fixed cells were blocked in PBS containing 0.1% Triton X-100 and 5% bovine serum albumin. For immunofluorescence, cells were incubated with the primary antibody overnight at 4°C. The cells were immunostained with an Alexa Fluor 488-conjugated secondary antibody in PBS for 2 h and the nuclei were counterstained with DAPI for 5 min at room temperature. For fluorescence, cells were stained with the nuclear counterstain DAPI for 5 min at room temperature after fixing. Fluorescent images were captured using a Leica TCS SP8 STED confocal microscope (Leica).

Mitochondria isolation

The mitochondria were isolated as previously described (12). The cells were washed at least thrice with cold PBS. The cell pellets were resuspended in the starting buffer (225 mM mannitol, 75 mM sucrose, 30 mM Tris–HCl, pH 7.4) and lysed using an ice-cold ULTRA-TURRAX Disperser (IKE). The cell lysates were centrifuged twice at 600 × *g* for 5 min each time at 4°C. Mitochondria were enriched in the pellet after being centrifuged at 7000 × *g* for 10 min at 4°C. The supernatant (cytoplasmic fraction) was centrifuged again to completely remove the mitochondrial components at 7000 × *g*. Mitochondria were centrifuged at 7000 × *g* for 10 min to purify the mitochondrial components. Mitochondria were completely lysed using radioimmunoprecipitation assay (RIPA) lysis buffer. All fractions (whole cell lysis, mitochondria, and cytoplasm) were added SDS loading buffer and boiled at 95°C for 10 min.

Nuclear isolation

The cells were washed at least thrice with cold PBS. The cell pellets were resuspended in NL buffer (10 mM 4-(2-hydroxyethyl)-1-piperazineethanesulfonic acid [pH 7.2], 1.5 mM $MgCl_2$, 10 mM KCl, 10 mM EDTA, and Proteinase inhibitor) and placed on ice for 15 min, followed by adding 25 μl 2% NP40 (final concentration 0.2%), and vortexing the cells at the maximum speed of the oscillator for 15 s. The lysate was centrifuged at 10 000 × *g* for 5 min at 4°C. The supernatant (cytoplasmic components) was centrifuged again to completely remove the nucleus components at 10 000 × *g* for 5 min at 4°C and the pellet (nucleus) was washed twice with 500 μl NL buffer (10 000 × *g*, 5 min, 4°C) and then lysed with 50 μl RIPA lysis buffer.

Northern blotting

RNA samples were separated on a 10% separating urea-gel in 0.1 M NaAc (pH 5.2) buffer at 4°C, 20 W for 20 h and then transferred to a positively charged nylon membrane at 4°C with 250 mA for 30 min in Tris-borated-EDTA (TBE) running buffer. The transformed membrane was ultraviolet-crosslinked at 3000 J/Cm^2. Then membrane was preblocked with a prehybridization solution (4 × saline-sodium citrate, 1 M Na_2HPO_4, 7% SDS, 1.5 × Denhardt solution, and 0.4 mg/l salmon sperm DNA) at 55°C for 1 h. 5′DIG (digoxin)-labeled probes (Supplementary Table S2) were used to hybridize the target tRNAs at 55°C overnight. The membrane was washed with washing buffer (0.1 M maleic acid and 0.15 M NaCl, pH 7.5) and blocked with blocking reagent (0.1 M maleic acid, 0.15 M NaCl, and 10% blocking reagent, pH 7.5) for 1 h at room temperature. The membrane was then incubated with an antibody buffer (blocking reagent and 1:10 000 anti-digoxigenin alkaline phosphatase) for 1 h and washed thrice for 15 min. The membrane was developed using CDP-Star

and imaged using an Amersham Imager 680 system (GE, CA, USA).

Construction of hAlaX KO cell lines

A sgRNA (5′-TGTTCAGTTCACCACCACCG-3′) was designed and inserted into the pX330-mcherry between BbsI sites. The vector was transfected into HEK293T cells using Lipofectamine 8000. After 48 h, single cells with mCherry fluorescent labels were sorted by flow cytometry (FACS Aria II, BD Biosciences), and single-cell clones were scaled up approximately 10 d later to identify whether hAlaX was knocked out using western blotting.

Dual-luciferase reporter assay

The 6 × AGC/AAA codons were inserted into the pmiroGLO plasmid after the firefly luciferase gene ATG start codon. The plasmid pmiroGLO-6xAGC or pmiroGLO-6xAAA plasmids were transfected into WT and KO cells (10# & 12#) in a 24-well plate using Lipofectamine 8000. After culturing for 24 h, the cells were harvested and assayed using the Dual-Glo Luciferase Assay System (Promega). Renilla luciferase was used to normalize firefly luciferase activity and to evaluate the translation efficiency of the reporter.

EGFP fluorescence intensity determination

pCMV-3Tag-3A constructs expressing EGFP and its S65 and A65 mutants were transfected into wild-type and KO cells (10# and 12#) in 96 well black plates (WHB, Shanghai, China) using Lipofectamine 8000. After cultivation for 24 h, the cells were washed thrice with PBS. Fluorescence intensity was detected at 395 and 488 nm using BioTek Synergy NEO and Gen 5.

Electrophoretic mobility shift assay (EMSA)

hAlaX (0–16 μM) and tRNA (0.2 μM) were incubated in 20 μl buffer (50 mM Tris–HCl (pH 6.8), 5 mM $MgCl_2$ and 5 mM KCl) at 4°C for 30 min at the absence or presence of 5 mM $ZnCl_2$. After incubation, 4 μl RNA loading buffer (0.25% bromophenol blue, 0.25% xylene cyanide and 60% glycerol) was added into each sample and loaded immediately on a 6% polyacrylamide native gel. The electrophoresis was performed on ice at a constant voltage of 90 V for 50 min. Ethidium bromide was used to stain the gels and detect shifts in tRNA.

Construction of *Sc*ΔAlaX

Two DNA segments containing the 5′untranslated region (UTR) (213 bp) and 3′UTR (287 bp) parts of the *Sc*AlaX gene were amplified from the BY4741 genome. 5′UTR and 3′UTR were digested with EcoRI and XhoI or BamHI and EcoRI and then simultaneously cloned into the pRS303 vector between the XhoI and BamHI sites. The plasmid pRS303-*Sc*AlaX-5′/3′UTR was linearized by EcoRI cleavage; the resultant linear vector was transformed into the BY4741 wild-type strain with Yeastmaker Yeast Transformation System 2 according to the manufacturer's protocol. Transformants were screened on a synthetic defined (SD)/His^- plate and selected for subsequent confirmation of loss of the *Sc*AlaX gene by polymerase chain reaction (PCR) and sequencing. The primers used are listed in Supplementary Table S1.

Yeast complementation

Genes encoding *Sc*AlaX and its mutants were ligated into the p425TEF-C-His_6. All constructs were transformed into *Sc*Δ*AlaX* using the Yeastmaker Yeast Transformation System 2 according to the manufacturer's protocol. Transformants were selected on SD/Leu^- plates, and a single clone was cultured in liquid SD/Leu^- medium at 30°C. The culture was diluted to a concentration equivalent to 1 optical density $(OD)_{600}$, and a 10-fold dilution series of the yeast cells was plated onto YPD (1% yeast extract, 2% peptone, 2% [v/v] glucose) and/or YPD with G418, cycloheximide (CHX), or other compounds/stressors. Complementation was observed by comparing the growth rates of *Sc*Δ*AlaX* expressing native *Sc*AlaX and its mutants. Yeast transformants were grown in liquid SD/Leu^- at 30°C and lysed following a previously described method (29,39).

Results

hAlaX is located exclusively in the cytoplasm

We overexpressed the gene encoding hAlaX with either a C-terminal FLAG tag (hAlaX-FLAG) or an enhanced green fluorescent protein (EGFP) tag (hAlaX-EGFP) in human embryonic kidney 293T (HEK293T) cells. Both proteins were readily detected at their expected molecular weights (MWs) (Supplementary Figure S1A). Immunofluorescence and fluorescence analyses revealed that hAlaX was predominantly localized in the cytoplasm. No clear signals were observed in the nuclei or mitochondria (Supplementary Figure S1B). We raised an anti-hAlaX antibody (anti-hAlaX) (Supplementary Figure S1C) from rabbits using purified hAlaX as the antigen. We then performed nuclear and cytoplasmic separation using wild-type HEK293T cells. Western blotting showed that hAlaX was absent in the nuclear fraction (Supplementary Figure S1D). To further exclude its potential presence in the mitochondria as a mitochondrial *trans*-editing factor, the mitochondrial fraction was isolated and western blotting revealed no distribution in the mitochondria (Supplementary Figure S1E). Taken together, these data suggest that hAlaX is a cytoplasmic protein that could edit cytoplasmic mischarged tRNAs, if it is able to do so.

Dimerization of hAlaX is mediated by the long helices between ED and C-Ala domains

Primary sequence alignments of hAlaX and various AlaRSs showed that hAlaX contains an ED domain and a C-Ala domain connected by two long helices. AlphaFold (40,41) predicted the three-dimensional (3D) structure of hAlaX with high confidence (per-residue confidence score > 90) (Figure 1A). This predicted hAlaX structure highly resembled the homologous part of *Archaeoglobus fulgidus* AlaRS (*Af*AlaRS) structure (Protein Data Bank [PDB]: 3WQY) (18), which is a dimer (Figure 1B) mediated by long helices.

We investigated whether hAlaX dimerizes *in vivo*. Genes encoding hAlaX-FLAG and C-terminal Myc-tagged hAlaX (hAlaX-Myc) were co-expressed in HEK293T cells, and co-immunoprecipitation (IP) (Co-IP) with anti-FLAG antibodies clearly showed that hAlaX-Myc could be pulled down (Figure 1C). Consistently, hAlaX-FLAG was readily co-precipitated using anti-Myc antibodies (Supplementary Figure S2A, lines 3 and 4). Consistent with a previous re-

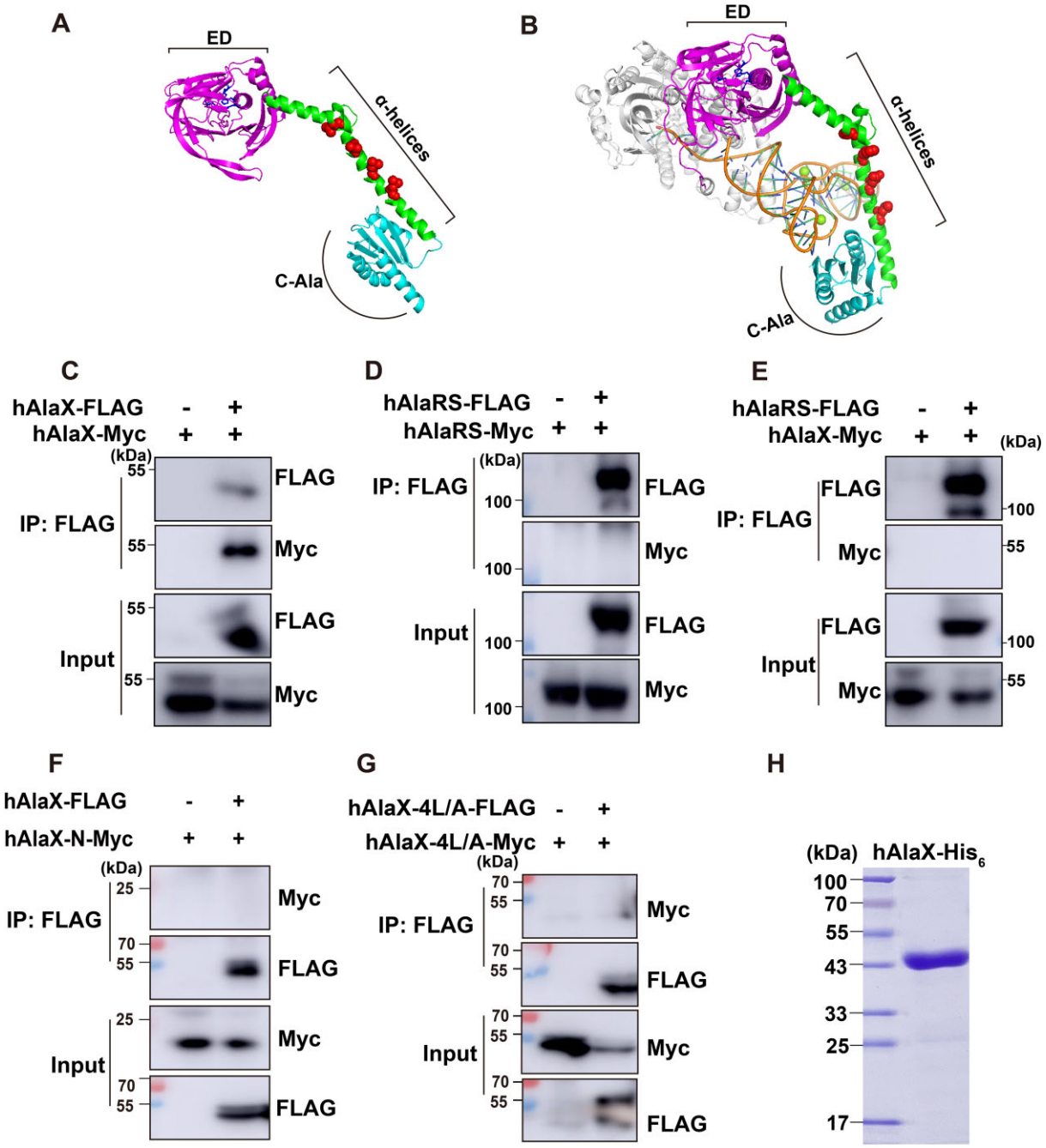

Figure 1. hAlaX is a dimer and does not interact with hAlaRS *in vivo*. (**A**) Structure of hAlaX predicted by AlphaFold (Identifier: AF-Q9BTE6-F1). (**B**) Co-crystal structure of *Af*AlaRS-tRNA^{Ala} (PDB: 3WQY); leucine zipper residues are highlighted in red in (A) and (B). (C–G) Analyses of interactions between hAlaX-FLAG and hAlaX-Myc (**C**), hAlaRS-FLAG and hAlaRS-Myc (**D**), hAlaRS-FLAG and hAlaX-Myc (**E**), hAlaX-FLAG and hAlaX-N-Myc (**F**) and hAlaX-4L/A-FLAG and hAlaX-4L/A-Myc (**G**) in HEK293T cells by co-immunoprecipitation using anti-FLAG antibodies. (**H**) SDS-PAGE of purified hAlaX (stained with Coomassie blue) from *E. coli*.

port (42), human cytoplasmic AlaRS (hAlaRS) existed as a monomer because FLAG-tagged AlaRS (hAlaRS-FLAG) and Myc-tagged hAlaRS (hAlaRS-Myc) could not be pulled down simultaneously (Figure 1D; Supplementary Figure S2A, lines 1 and 2). Considering that the long helices between the ED and C-Ala domains in bacterial and archaeal AlaRSs are responsible for homodimerization (18), we investigated whether hAlaX and hAlaRS (both containing long helices) interact in the cytoplasm. For this purpose, genes encoding hAlaRS-FLAG and hAlaX-Myc were co-expressed, and Co-IP assays revealed no interaction using either anti-FLAG (Figure 1E) or anti-Myc (Supplementary Figure S2A, lines 5 and 6) antibodies. These results show that hAlaX was able to dimerize but did not interact with AlaRS *in vivo*.

We further explored whether the long helices mediate hAlaX dimer formation. We co-expressed genes encoding hAlaX-FLAG and a Myc-tagged N-terminal ED domain (Met^{1}-Gly^{243}, containing only the ED domain) (hAlaX-N-Myc) in HEK293T cells. Co-IP assays revealed no interaction be-

tween hAlaX-FLAG and hAlaX-N-Myc using either anti-FLAG or anti-Myc antibodies (Figure 1F, Supplementary Figure S2B), suggesting that the hAlaX helices are likely responsible for dimerization. Alignment of primary sequences revealed the presence of a stretch of putative leucine zipper residues in the helices (L260, L278, L285 and L292), which were (semi-) conserved among various AlaXs and even archaeal *Af*AlaRS (Supplementary Figure S2C). All their counterparts in *Af*AlaRS (L751, V769, W776 and I783) constitute the dimerization interface, as revealed in the *Af*AlaRS structures (PDB: 3WQY, 2ZVF) (18,43). The four Leu residues were simultaneously replaced with Ala in the resultant mutant hAlaX-4L/A. Co-IP analysis revealed that the overexpressed hAlaX-4L/A-FLAG and hAlaX-4L/A-Myc failed to dimerize (Figure 1G).

Altogether, the above data show that hAlaX dimerizes *in vitro* and *in vivo*. Dimerization is mediated by hydrophobic interactions via leucine zippers in the long connecting helices between the ED and C-Ala domains.

hAlaX is an active *trans*-editing factor with Ser specificity

To explore the putative *trans*-editing activity of hAlaX, we performed hydrolysis of Ser-tRNA^{Ala} (prepared from *E. coli* editing-deficient mutant C666A, *Ec*AlaRS-C666A) (44). Recombinant hAlaX was obtained from *E. coli* expression system (Figure 1H). hAlaX was able to cleave Ser-tRNA^{Ala} (Supplementary Figures S3A, B). To explore the amino acid specificity during editing, we prepared Ala-tRNA^{Ala} and Gly-tRNA^{Ala} using *Ec*AlaRS-C666A. Hydrolysis of these two (mis)charged tRNAs showed that hAlaX was unable to efficiently hydrolyze Ala- or Gly-tRNA^{Ala} (Supplementary Figures S3C–F). Consistent with a previous report (14), Gly-tRNA^{Ala} was rapidly hydrolyzed by human DTD (hDTD1) (Supplementary Figures S3G, H), indicating a good quality of the prepared mischarged tRNA. These data show that hAlaX is an active *trans*-editing factor with amino acid specificity for clearing Ser-tRNA^{Ala}*in vitro*.

hAlaX has the relaxed tRNA specificity to hydrolyze nearly all Ser-(mis)charged tRNAs

Based on the cytoplasmic distribution and editing capacity of hAlaX, and to better understand whether Ser-tRNA^{Ala} is the sole editing substrate of hAlaX, we prepared other Ser-(mis)charged cytoplasmic tRNAs. These were Ser-tRNA^{Ser} (aminoacylation product of SerRS), Ser-tRNA^{Thr} (misaminoacylation product of ThrRS) and Ser-tRNA^{Sec} (intermediate in Sec-tRNA^{Sec} biogenesis by SerRS), all of which are naturally charged tRNAs found in mammalian cells (Supplementary Figure S4). hAlaX was able to substantially edit all these tRNA species, suggesting that hAlaX readily recognizes tRNA^{Ser}, tRNA^{Thr} and tRNA^{Sec} (Figure 2; Supplementary Figures S5A–D). However, hydrolysis of Thr-tRNA^{Thr} (aminoacylation product of ThrRS) (Supplementary Figure S4B) by hAlaX was not obviously observed (Supplementary Figures S5E, F), confirming that hAlaX displayed specificity only toward Ser. To further understand whether hAlaX exhibits a relaxed tRNA specificity, we prepared various Ser-(mis)charged mitochondrial tRNAs (mtRNAs) using native or editing-defective mitochondrial (mt) aaRSs, including Ser-mtRNA^{Thr} (misaminoacylation product of mtThrRS, prepared by mtThrRS-H131A/H133A) (45), Ser-mtRNA^{Ala} (misaminoacylation product of mtAlaRS, prepared by mtAlaRS-C749A) (30), and Ser-mtRNA^{Ser}(AGY) (aminoacylation product of mtSerRS) (46) (Supplementary Figure S6). Editing assays showed that hAlaX robustly removed Ser from Ser-mtRNA^{Thr} and Ser-mtRNA^{Ser}(AGY) (Supplementary Figures S7A–D); however, Ser-mtRNA^{Ala} appeared to be the only mischarged tRNA that was not hydrolyzed by hAlaX (Supplementary Figures S7E, F).

These results revealed that hAlaX harbors an inherent ability to hydrolyze all Ser-ligated tRNAs, except Ser-mtRNA^{Ala}. Mitochondrial tRNA^{Ser}(AGY) is unique in all human tRNAs being a truncated tRNA with a 'Y'- rather than 'L'-shaped 3D architecture (47). Moreover, tRNA^{Sec} is also a peculiar tRNA with a 9 + 4 instead of canonical 7 + 5 mode of minihelix containing amino acid acceptor plus TψC stems (48). These results demonstrate that hAlaX does not exhibit sequence-specific tRNA specificity during editing.

hAlaX recognizes tRNAs independently of the L-shaped-structure and the sequence of the acceptor stem

The ability of hAlaX to edit Ser-mtRNA^{Ser}(AGY) suggests that a canonical tRNA L-shaped structure is not a prerequisite for recognition, as mtRNA^{Ser}(AGY) lacks a D-arm. However, AlaRS-tRNA^{Ala} structures have shown that a Gly-rich peptide in the C-Ala domain is responsible for binding to the elbow region of tRNA^{Ala} during aminoacylation and editing (17,18). In particular, Gly-rich peptides are conserved in mammalian AlaXs. As shown, Ser-tRNA^{Ser} is an excellent editing substrate for hAlaX (Figure 2). In addition, the preparation of the aminoacylation products of tRNA^{Ser} variants by SerRS is highly efficient and convenient because tRNA^{Ser} aminoacylation primarily relies on the discriminator base and long variable arm (49). Therefore, we used Ser-tRNA^{Ser} to investigate the substrate recognition mechanism of hAlaX.

In tRNA^{Ser}(AGA) folding, the conserved G18 and G19 residues interact with U55 and C56, respectively, to maintain the integrity of the elbow region (50). Therefore, to investigate the role of the L-shaped structure during hAlaX editing, we first introduced two mutations in the elbow region, including the construction of single-point mutants, tRNA^{Ser}(AGA)-G19C (disruption of the G19-C56 interaction), and tRNA^{Ser}(AGA)-U55A (disruption of the G18-U55 interaction) (Supplementary Figure S8). Both the mutants were efficiently charged with SerRS. Editing assays showed that hAlaX robustly hydrolyzed Ser-tRNA^{Ser}(AGA)-G19C (Figure 3A) and Ser-tRNA^{Ser}(AGA)-U55A (Figure 3B). To disrupt the putative inter-domain base pairing in the elbow region more severely, we constructed a double-point mutant (tRNA^{Ser}(AGA)-C18-A56 mutant, with disruption of both G18-U55 and G19-C56 interactions) (Supplementary Figure S8). In addition, we also deleted the loop region bases ^{55}UCGAA^{59} (ΔTψC) (Supplementary Figure S8) to break the L-shaped structure. Hydrolysis results showed that both Ser-tRNA^{Ser}(AGA)-C18-A56 (Figure 3C) and Ser-tRNA^{Ser}(AGA)-ΔTψC (Figure 3D) were good substrates for hAlaX, demonstrating that an L-shaped-structure is not a prerequisite for editing.

Ser-mtRNA^{Ala} was the only Ser-mischarged tRNA that was not cleared by hAlaX (Supplementary Figures S7E, F). Since the amino acid acceptor stem is the region that

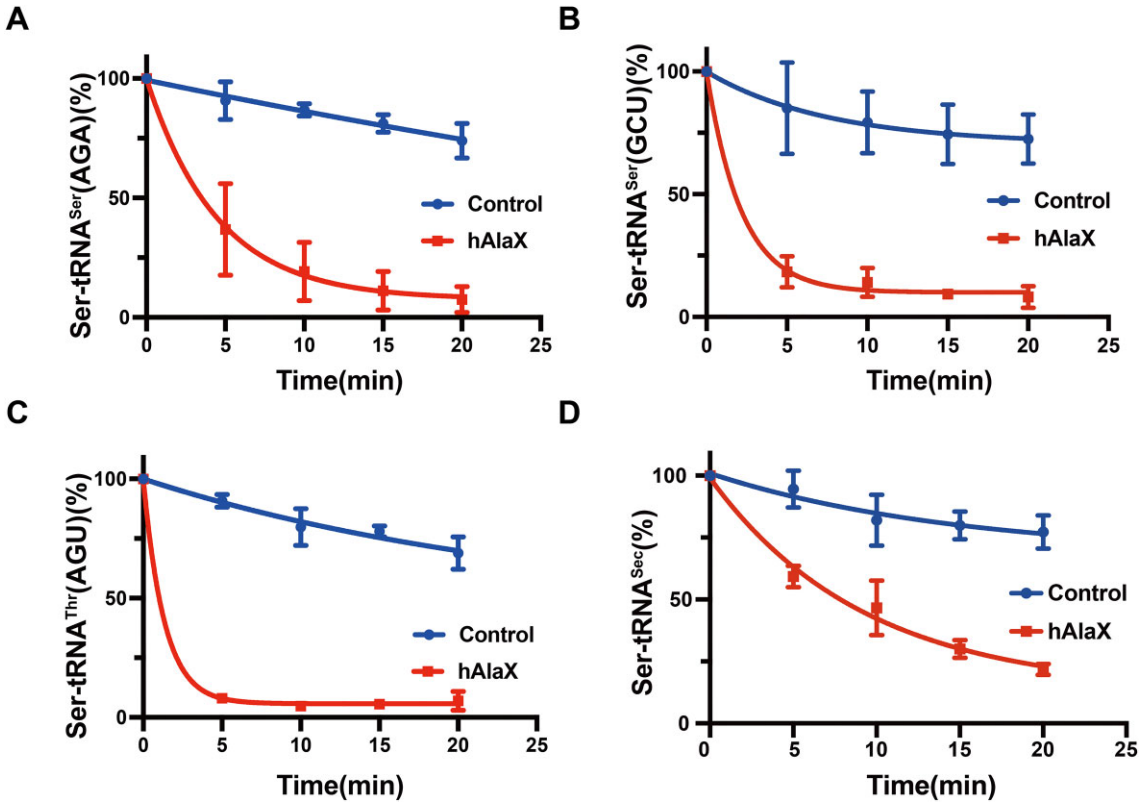

Figure 2. hAlaX hydrolyzes all cytoplasmic Ser-(mis)charged tRNAs. Editing activity of hAlaX (red line) against Ser-[^{32}P]tRNA^{Ser}(AGA) (**A**), Ser-[^{32}P]tRNA^{Ser}(GCU) (**B**), Ser-[^{32}P]tRNA^{Thr}(AGU) (**C**) and Ser-[^{32}P]tRNA^{Sec} (**D**). The control reaction (blue line) represents spontaneous hydrolysis of aa-[^{32}P]tRNA without the addition of hAlaX. Data represent mean ± standard deviation (SD) ($n = 3$).

interacts most with the ED domain of AlaRS (18), we compared the amino acid acceptor stem sequence of mtRNA^{Ala} with those of other tRNAs, including tRNA^{Ser}, tRNA^{Ala}, tRNA^{Thr}, tRNA^{Sec}, mtRNA^{Ser}(AGY), and mtRNA^{Thr} (Figure 3E). No consensus base pairs were found except G1-C72 in hAlaX substrate tRNAs *vs*. A1-U72 in mtRNA^{Ala}. To understand whether G1-C72 functions as a key element in hAlaX editing, we mutated tRNA^{Ser}(AGA) G1-C72 to G1-U72 and U1-G72 (Figure 3E). Both Ser-mischarged tRNA^{Ser} mutants were efficiently hydrolyzed by hAlaX (Figure 3F, Supplementary Figure S9A). Furthermore, we substituted A1-U72 in mtRNA^{Ala} with G1-C72 (Figure 3E). hAlaX did not hydrolyze Ser-mtRNA^{Ala}(G1-C72) (Figure 3G).

The most peculiar feature of mtRNA^{Ala} is the presence of G3-C70, but not G3-U70 (Figure 3F), which is unique and absolutely conserved in other tRNA^{Ala}s (30). We mutated the C70 in mtRNA^{Ala} to U70 and prepared Ser-mtRNA^{Ala}-U70. hAlaX gained the capacity to hydrolyze Ser-mtRNA^{Ala}-U70 (Supplementary Figure S9B). However, the lack of G3-U70 in tRNA^{Ser}, tRNA^{Thr}, and tRNA^{Sec} (Figure 3E) suggests that G3-U70 is not a positive recognition element for hAlaX. The gain of editing after introduction of G3-U70 suggests that natural G3-C70 refines the local conformation of mtRNA^{Ala}, making its CCA-terminus inaccessible to the editing pocket of hAlaX. A similar mechanism of conformational regulation by G3-C70 has been observed in *Af*AlaRS-tRNA^{Ala} structures (PDB: 3WQY and 3WQZ) (18).

Altogether, the above data suggest that hAlaX recognizes tRNAs in an acceptor stem sequence-independent manner and does not depend on an intact tRNA L-shaped structure.

Editing by hAlaX is sensitive to Zn^{2+} concentrations or mutations in the conserved Gly-rich motif in the C-Ala domain

The editing active sites of AlaRS and ThrRS comprise two conserved motifs, HXXXH and CXXXH, which form a zinc-finger (ZF) motif (23,51). This ZF motif is also conserved in AlaXs (Supplementary Figures S10A, B) and is essential for editing of AlaRS and ThrRS (11,29,52,53). We mutated C209 in the CXXXH motif of hAlaX to Ala (Supplementary Figures S10A, B). hAlaX-C209A was defective in catalysis (Supplementary Figure S10C), demonstrating the importance of the ZF motif for hAlaX editing. Upon optimizing the reaction conditions, we found that increasing the Zn^{2+} concentration gradually inhibited the editing activity of hAlaX, which was abolished in the presence of 200 μM $ZnCl_2$ (Supplementary Figure S10D). However, even in the presence of millimolar Zn^{2+}, tRNA was still efficiently bound by hAlaX (Supplementary Figure S10E), suggesting that the inhibitory effect of excess Zn^{2+} was not due to reduced tRNA binding, but to impaired catalysis. However, the detailed mechanism of the inhibitory effect of excess Zn^{2+} requires further study.

In all AlaRS/AlaX-L proteins, the C-Ala domain is the most structurally conserved domain, albeit with sequence divergence (17,18,26) (Figure 1A). AlphaFold predicts that hAlaX is composed of a five-stranded β-sheet and three surrounding α-helices (Figure 1A, Supplementary Figures S10F, G). Notably, a conserved Gly-rich motif is present in bacterial and eukaryotic AlaRSs which is thought to bind to the tRNA elbow region (17,54). This Gly-rich motif constitutes peptide ^{375}GKGAGK^{380} in the β5 strand of hAlaX

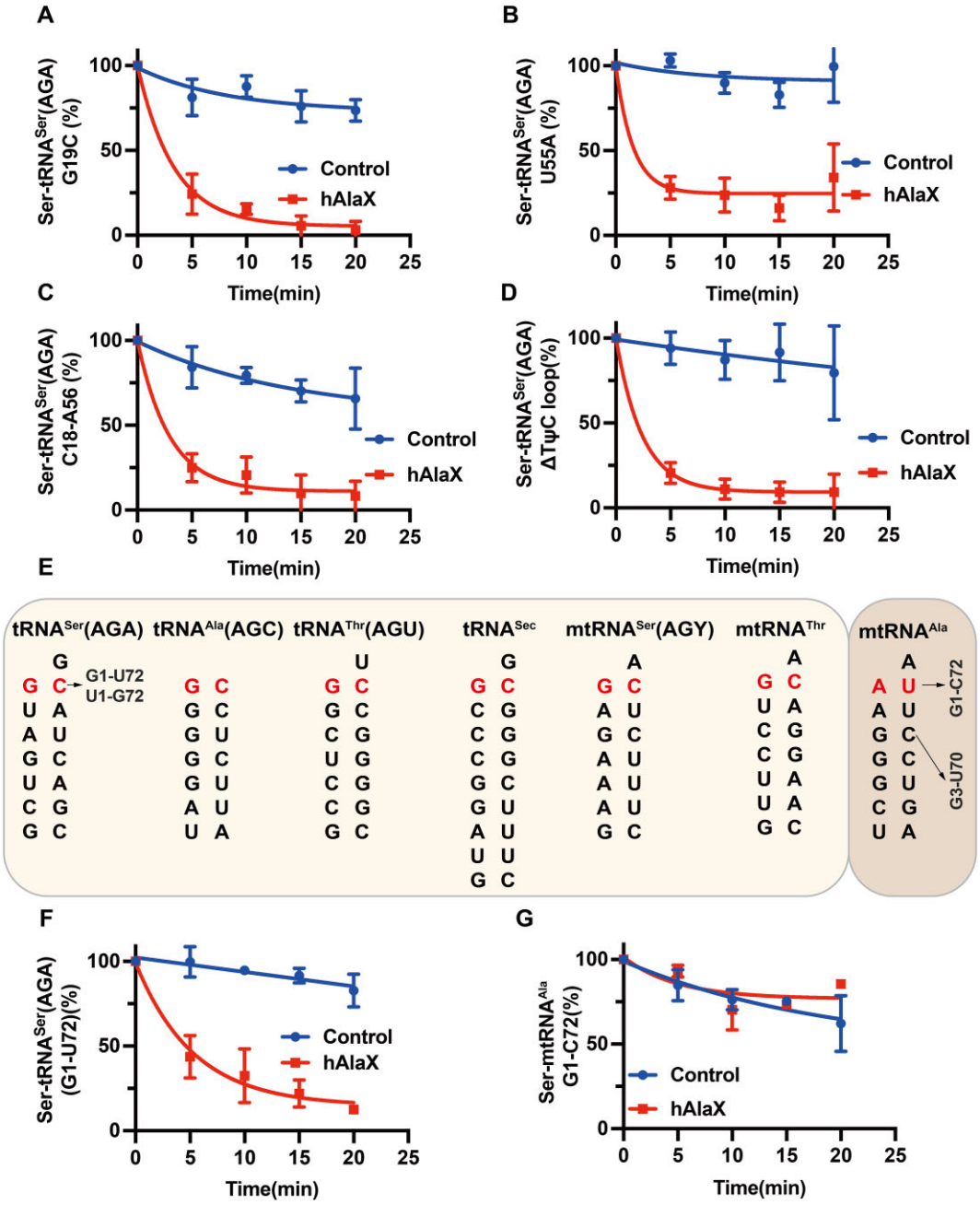

Figure 3. hAlaX recognizes tRNAs in a L-shaped structure in an amino acid acceptor stem sequence-independent manner. (**A**) Editing activity of hAlaX (red line) against Ser-[^{32}P]tRNA^{Ser}(AGA)-G19C (**A**), Ser-[^{32}P]tRNA^{Ser}(AGA)-U55A (**B**), Ser-[^{32}P]tRNA^{Ser}(AGA)-C18-A56 (**C**), Ser-[^{32}P]tRNA^{Ser}(AGA)-ΔTψC-loop (**D**). (**E**) Sequence comparison among acceptor stems of various tRNAs. Mutations introduced into tRNA^{Ser}(AGA) and mtRNA^{Ala} are indicated. Editing activity of hAlaX (red line) against Ser-[^{32}P]tRNA^{Ser}(AGA)-G1-U72 (**F**) and Ser-[^{32}P]mtRNA^{Ser}(AGY)-G1-C72 (**G**). In all relevant curves, a control reaction (blue line) represents the spontaneous hydrolysis of aa-[^{32}P]tRNA without hAlaX addition. Data represent mean ± SD ($n = 3$).

(Supplementary Figure S10F). We replaced G377 with Leu to introduce a longer side chain. Besides, we mutated K380 to Ala to alter the size and charge of the side chain. Hydrolysis of Ser-tRNA^{Ser} showed that hAlaX-K380A exhibited impaired editing activity, whereas that of hAlaX-G377L was abolished (Supplementary Figure S10H). These structural and biochemical analyses revealed that the C-Ala domain, especially its conserved Gly-rich motif, is essential for *trans*-editing of hAlaX. These data also imply that some elements of the tRNA elbow region are recognized by the C-Ala domain, although disruption of the interaction between the D- and T-loops has a negligible effect on hAlaX editing (Figures 3A-D). Moreover, considering the non-cannonical binding of tRNA T-stem by human mitochondiral AlaRS (55), potential interaction between C-Ala of hAlaX with other part of tRNA (such as the T-stem) is also possible.

Editing multiple Ser-(mis)charged tRNAs is an evolutionarily conserved activity of eukaryotic AlaX

*Sc*AlaX has the same domain organization as hAlaX (Supplementary Figure S11A). The putative active-site

residues of *Sc*AlaX (^{125}HXXXH^{129} and ^{240}CXXXH^{244}) are conserved (Supplementary Figures S10A, S11A). Moreover, conserved leucine-zipper residues in the long helices and a Gly-rich motif in the C-Ala domain are also present (Supplementary Figures S2C, S10F). We purified *Sc*AlaX from *E. coli* overexpression system (Supplementary Figure S11B). Our results revealed that Ser-tRNA^{Ala}(AGC) was efficiently cleared by *Sc*AlaX (Figure 4A, Supplementary Figure S11C), demonstrating that *Sc*AlaX is not inactive, as previously reported (27) but is an active *trans*-editing factor, consistent with another report (19). Based on the wide substrate specificity of hAlaX, we investigated whether *Sc*AlaX could hydrolyze Ser-tRNA^{Thr} and Ser-tRNA^{Ser}. Both (mis)charged tRNA species were hydrolyzed by *Sc*AlaX (Figures 4B, C, Supplementary Figures S11D, E). To confirm that the decreased amount of (mis)charged tRNAs was due to the editing function of *Sc*AlaX, C240 in ^{240}CXXXH^{244} motif (Supplementary Figure S9A) was mutated to Ala. The resulting *Sc*AlaX-C240A exhibited almost no editing activity for Ser-tRNA^{Ser} (Figure 4D, Supplementary Figure S11F).

Collectively, our results demonstrate that *Sc*AlaX is an active *trans*-editing factor *in vitro* and exhibits multiple substrate specificities similar to hAlaX, suggesting that editing multiple Ser-(mis)charged tRNAs is an evolutionarily conserved activity of eukaryotic AlaXs.

Editing function of *Sc*AlaX for Ser-tRNA^{Ala} or Ser-tRNA^{Thr} *in vivo* regulated yeast growth under geneticin sulfate (G418) and cycloheximide (CHX) stresses

To monitor the putative *in vivo* editing activity of *Sc*AlaX, we constructed *Sc*AlaX gene knockout BY4741 strain (*Sc*ΔAlaX) via homologous recombination (Supplementary Figure S12A, B). The resulting *Sc*ΔAlaX strain exhibited no obvious growth defects on yeast extract peptone dextrose (YPD) plates under physiological culture conditions (Supplementary Figure S12C). Thus, we further compared growth of wild-type and *Sc*ΔAlaX strains under different stresses, including higher salt (200 mM NaCl), oxidative stress (5 mM H_2O_2), altering plasma membrane fluidity (8% EtOH), inhibiting protein synthesis (10 μM chloramphenicol (Cm) or 10 μg/ml puromycin), blocking proteasome degradation (50 μM MG132) at the absence or presence of 40 mM Ser, considering that excessive Ser would potentially pose a higher threat to translation accuracy given Ser specificity of *Sc*AlaX editing. However, in the presence of all stress factors, the two yeast strains developed with comparable efficiency (Supplementary Figure S12C). In additional efforts, we unexpectedly found that *Sc*ΔAlaX could tolerate a high concentration (200 μg/ml) of G418, which is an aminoglycoside antibiotic that inhibits nearly every step of protein synthesis (initiation, elongation, termination, and recycling) by binding multiples sites of the ribosome (56) (Figure 5A). To detect whether this unexpected gain of function in growth is caused by the deletion of *Sc*AlaX gene rather than off-target homologous recombination, we reintroduced wild-type *Sc*AlaX gene to *Sc*ΔAlaX and found that growth sensitivity to G418 was regained (Figure 5B). However, introducing an empty p425TEF vector failed to confer G418-sensitivity of *Sc*ΔAlaX. To confirm that growth tolerance of G418 is due to the loss of editing function of *Sc*AlaX, the editing deficient *Sc*AlaX-C240A was overexpressed in *Sc*ΔAlaX (Supplementary Figure S12D). However, *Sc*AlaX-C240A failed to restore G418-sensitivity of *Sc*ΔAlaX (Figure 5B). These results show that yeast tolerance to the inhibitory effect of G418 is caused by the loss of *Sc*AlaX editing activity.

Given editing of two Ser-mischarged tRNAs *in vitro* by *Sc*AlaX, G418-resistance of *Sc*ΔAlaX implies that generation of Ser-tRNA^{Ala} or Ser-tRNA^{Thr} can antagonize the multiple inhibitory effects of G418. To explore this possibility, we overexpressed the gene encoding *S. cerevisiae* cytoplasmic AlaRS (*Sc*AlaRS) or cytoplasmic ThrRS (*Sc*ThrRS) in *Sc*ΔAlaX, and subsequent growth observation showed that overexpression of either tRNA synthetase was able to restore the growth sensitivity to G418 (Figures 5C, D, Supplementary Figure S12D). We further mutated the conserved editing active site C719 in *Sc*AlaRS (53) or H151 and H155 in *Sc*ThrRS (29) to disrupt the editing activity. In sharp contrast, editing deficient *Sc*AlaRS-C719A or *Sc*ThrRS-H151A/H155A (*Sc*ThrRS-HH) were unable to rescue G418-sensitivity of *Sc*ΔAlaX (Figures 5C, D). The gain of G418-resistance after loss of *Sc*AlaX and complementation assays suggest that (1) *Sc*AlaX is active in editing Ser-tRNA^{Ala} and Ser-tRNA^{Thr}*in vivo*; (2) loss of *Sc*AlaX editing favours yeast to counteract the inhibitory effects of G418; and (3) increased *cis*-editing by the corresponding tRNA synthetase can compensate for the loss of *Sc*AlaX *trans*-editing activity.

Given the gain of resistance toward G418, a translational inhibitor, we tested the growth of yeast in the presence of different concentrations of CHX, another protein synthesis inhibitor that interferes with translation elongation (57). Wild-type yeast exhibited more robust growth than *Sc*ΔAlaX in the presence of 0.3 μg/ml CHX (Supplementary Figure S13A). Inhibitory growth of *Sc*ΔAlaX strain by CHX was ameliorated by expression of wild-type *Sc*AlaX, *Sc*AlaRS or *Sc*ThrRS but not by editing deficient *Sc*AlaX-C240A, *Sc*AlaRS-C719A or *Sc*ThrRS-HH (Supplementary Figure S13B–D).

To directly detect possible translation errors in the *Sc*ΔAlaX strain, we overexpressed editing-deficient His_6-tagged *Sc*ThrRS-HH in wild-type and *Sc*ΔAlaX strains. After purification by Ni-nitrilotriacetic acid affinity chromatography, enriched samples from the two strains were separated by sodium dodecyl-sulfate polyacrylamide gel electrophoresis (SDS-PAGE) and silver stained. A single band of approximately 84 kDa from each sample, corresponding to the MW of *Sc*ThrRS-HH-His_6, was analyzed using liquid chromatography–tandem mass spectrometry (LC–MS/MS). For the wild-type strain, 60 *Sc*ThrRS-HH peptides were captured without Ala-to-Ser or Thr-to-Ser incorporation errors. In contrast, of the 97 *Sc*ThrRS-HH peptides sequenced in the *Sc*ΔAlaX sample, three peptides containing two Ala-to-Ser and one Thr-to-Ser misincorporation errors were identified (Figure 5E, Supplementary Figure S14). These results show that the loss of *Sc*AlaX activity triggers Ser replacement at the Ala or Thr codons in yeast.

Altogether, despite rationale for distinct responses of *Sc*ΔAlaX to different translational inhibitors (no responses to Cm and puromycin, resistance to G418, and sensitivity to CHX) is currently unknown; however, complementation of growth alterations with G418 and CHX by editing-competent *Sc*AlaX, *Sc*AlaRS, or *Sc*ThrRS and the identification of Ser translation errors at Ala or Thr codons in *Sc*ΔAlaX yeast, demonstrates that *Sc*AlaX is an active *trans*-editing factor for Ser-tRNA^{Ala} and Ser-tRNA^{Thr}*in vivo*.

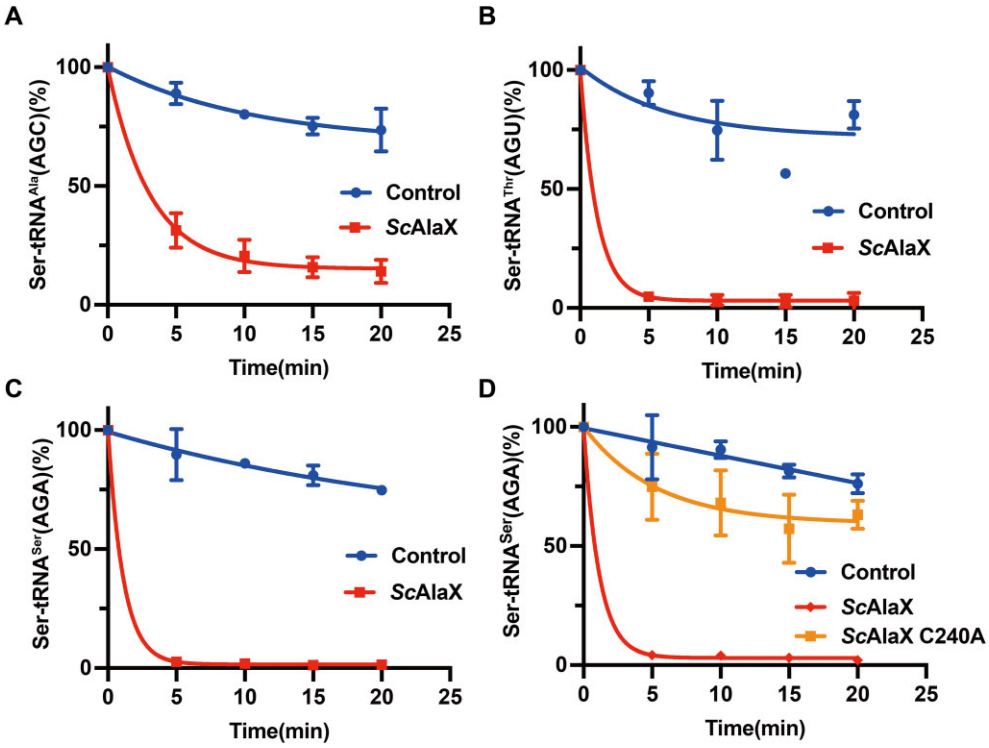

Figure 4. *Sc*AlaX is an active *trans*-editing factor that hydrolyzes multiple Ser-(mis)charged tRNAs *in vitro*. Editing activity of *Sc*AlaX (red line) against Ser-[^{32}P]tRNA^{Ala}(AGC) (**A**), Ser-[^{32}P]tRNA^{Thr}(AGU) (**B**), and Ser-[^{32}P]tRNA^{Ser}(AGA) (**C**). (**D**) Editing activity of *Sc*AlaX (red line) and *Sc*AlaX-C240A (orange line) against Ser-[^{32}P]tRNA^{Ser}(AGA). The control reaction represents the spontaneous hydrolysis of aa-[^{32}P] tRNA without enzyme addition. Data represent mean ± SD ($n = 3$).

hAlaX served as the third layer of proofreader for AlaRS and ThrRS in mammalian cells

The yeast data revealed the hydrolysis of Ser-tRNA^{Ala} and Ser-tRNA^{Thr} by *Sc*AlaX *in vivo*. To determine whether hAlaX can hydrolyze Ser-mischarged tRNAs in mammalian cells, we deleted the hAlaX gene (*AARSD1*) in HEK293T cells using the clustered regularly interspaced short palindromic repeats (CRISPR)-CRISPR associated protein 9 (Cas9) gene editing technology with single guide RNA targeting exon 2 (Supplementary Figure S15A). Two knock-out (KO) cell lines (10# & 12#) with frameshift mutations in both alleles were obtained (Supplementary Figure S15B). No endogenous hAlaX was detected in either cell line using western blotting (Supplementary Figure S15C).

Aminoacylation levels of tRNA^{Ala} and tRNA^{Thr} in wild-type HEK293T cells and the two KO cell lines were determined by northern blotting under acidic conditions that preserve the ester bond of charged tRNAs. No significant differences of charging levels of tRNA^{Ala} and tRNA^{Thr} between wild-type and KO cells were observed (Supplementary Figures S15D, E). The absence of detectable differences in tRNA^{Ala} or tRNA^{Thr} charging levels could be due to several reasons. Ser misactivation by AlaRS or ThrRS may be rare compared with activation of the cognate Ala or Thr. For instance, the discriminator factors of mammalian and yeast ThrRSs for Ser in Thr selection are 1/1033 and 1/910, respectively (29,32). Similarly, the discriminator factor of mammalian AlaRSs for Ser in Ala selection is 1/569 (30). A low level of misactivation suggests that only trace amounts of Ser-mischarged tRNA^{Ala} or tRNA^{Thr} exist in cellular pools of aminoacyl-tRNAs. In addition, AlaRS or ThrRS hydrolyze a substantial proportion of Ser-mischarged tRNA^{Ala} or tRNA^{Thr} via *cis*-editing. These two mechanisms leave only a minimal ratio of Ser-mischarged tRNA^{Ala} or tRNA^{Thr} waiting to be *trans*-edited by hAlaX. This suggests that the sensitivity of acidic northern blotting is insufficient to detect such trace amounts of hydrolysis of Ser-mischarged tRNAs and therefore no significant alteration in the level of tRNA^{Ala} or tRNA^{Thr} charging is detectable as observed here. Consequently, we looked for other methods to explore the potential editing of Ser-mischarged tRNAs *in vivo*.

Previous studies have reported that the major excitation peak of EGFP shifts from 488 to 395 nm when the protein sequence ^{65}AYG^{67} or ^{65}TYG^{67} is mutated to ^{65}SYG^{67} (58,59). We confirmed the excitation spectra of wild-type EGFP (containing T65) and its S65 and A65 mutants by overexpressing individual EGFP in wild-type HEK293T cells. Fluorescence spectrum monitoring showed that the major excitation peak of EGFP-S65 was at 395 nm, whereas that of wild-type EGFP (T65) or the A65 mutant was near 488 nm (Supplementary Figure S16A). Accordingly, when excited at 395 and 488 nm, an obvious difference in fluorescence intensity was observed for EGFP-S65, which was bright at 395 nm, but showed lesser fluorescence at 488 nm (Supplementary Figure S16B). By utilizing this selective excitation of S65-containing EGFP at 395 nm, we overexpressed either wild-type EGFP (T65) or the EGFP-A65 mutant in wild-type and KO cell lines (10# & 12#). Theoretically, if hAlaX can deacylate Ser-tRNA^{Ala} or Ser-tRNA^{Thr}, the loss of hAlaX should result in misincorporation of Ser at the Ala or Thr codons, stimulating a higher excitation level at 395 nm (Supplementary Figure S16C). The results showed that, after subtraction of negligible background fluorescence, the relative fluorescence intensity (395 nm/488 nm,

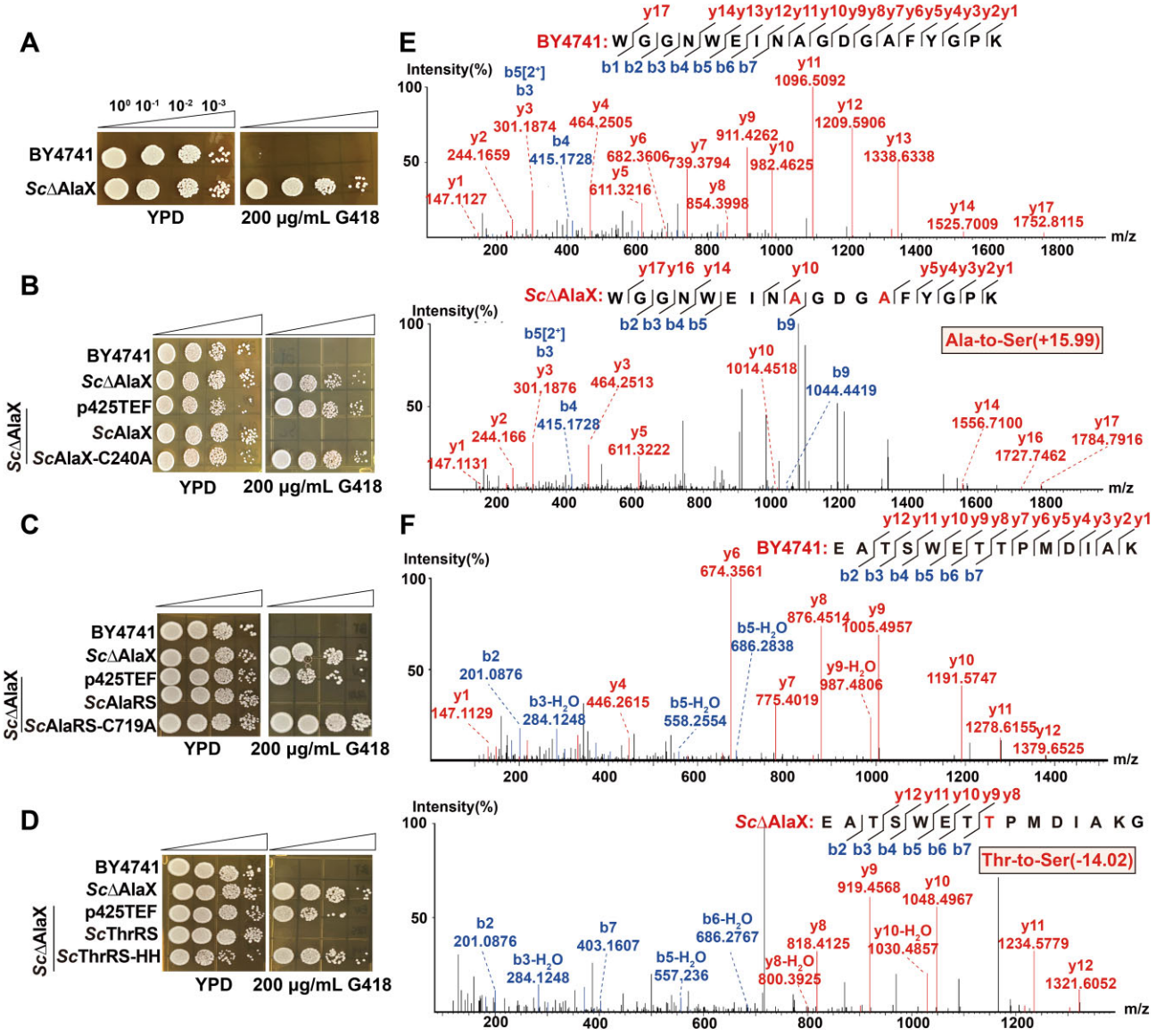

Figure 5. *Sc*AlaX is an active *trans*-editing factor *in vivo*. (**A**) Growth phenotypes of wild-type BY4741 and *Sc*ΔAlaX strains in YPD and YPD at presence of 200 μg/ml G418. (**B**) Complementation phenotype of *Sc*AlaX and *Sc*AlaX-C240A. (**C**) Complementation phenotype of *Sc*AlaRS and *Sc*AlaRS-C719A. (**D**) Complementation phenotype of *Sc*ThrRS and *Sc*ThrRS-HH. In all complementation assays, the empty p425TEF and *Sc*AlaX were introduced as negative and positive controls, respectively. (**E**) LC–MS/MS analysis of enriched *Sc*ThrRS-HH from wild-type BY4741 (upper) and *Sc*ΔAlaX (lower) strains. Two Ala-to-Ser misincorporation occurrences are indicated by the red A. (**F**) LC–MS/MS analysis of enriched *Sc*ThrRS-HH from wild-type BY4741 (upper) and *Sc*ΔAlaX (lower) strains. One Thr-to-Ser misincorporation occurrence is indicated by the red T.

calculated using the excitation values in the same sample and thus not influenced by EGFP levels among different cell lines) in the two KO cell lines expressing wild-type EGFP (T65) or EGFP-A65 was significantly higher than that in the wild-type cells (Figure 6A), indicating that there was more Ala-to-Ser or Thr-to-Ser mistranslation at position 65 in EGFP. However, no elevated (in fact, a little reduced) fluorescence intensity was observed when EGFP-S65 was overexpressed in wild-type or KO cell lines (Figure 6A).

To directly observe Ser-tRNA^{Ala} or Ser-tRNA^{Thr} hydrolysis, we performed MS analysis in wild-type and KO (10# & 12#) cells. We overexpressed C-terminal FLAG-tagged EGFP (EGFP-FLAG) in wild-type HEK293T and KO cells (10# & 12#) and then enriched it by IP using anti-FLAG antibodies. Purified EGFP-FLAG was digested and analyzed by LC–MS/MS to detect Ser misincorporation. In total, 100 EGFP-derived peptides were detected in enriched EGFP samples from wild-type cells, and two identical fragments (^{86}SAMPEGYVQER^{96}) harbored an Ala-to-Ser misincorporation (underlined), which was also found in enriched EGFP samples from both KO cell lines, suggesting that A87 is an error-prone decoding site for EGFP mRNA translation in all cell lines. No other misincorporation was identified in EGFP from wild-type cells. However, among the 111 EGFP-derived peptides from KO 12# cells, in addition to the shared mistranslated peptide (^{86}SAMPEGYVQER^{96}), two additional peptides harbored two Thr-to-Ser and one Ala-to-Ser misincorporations, which were otherwise native to EGFP from wild-type cells (Figure 6B, C). Similarly, of the 76 EGFP-derived peptides from KO 10# cells, in addition to the shared mistranslated peptide (^{86}SAMPEGYVQER^{96}), two additional peptides contained a misincorporation of Ala-to-Ser or Thr-to-Ser. The

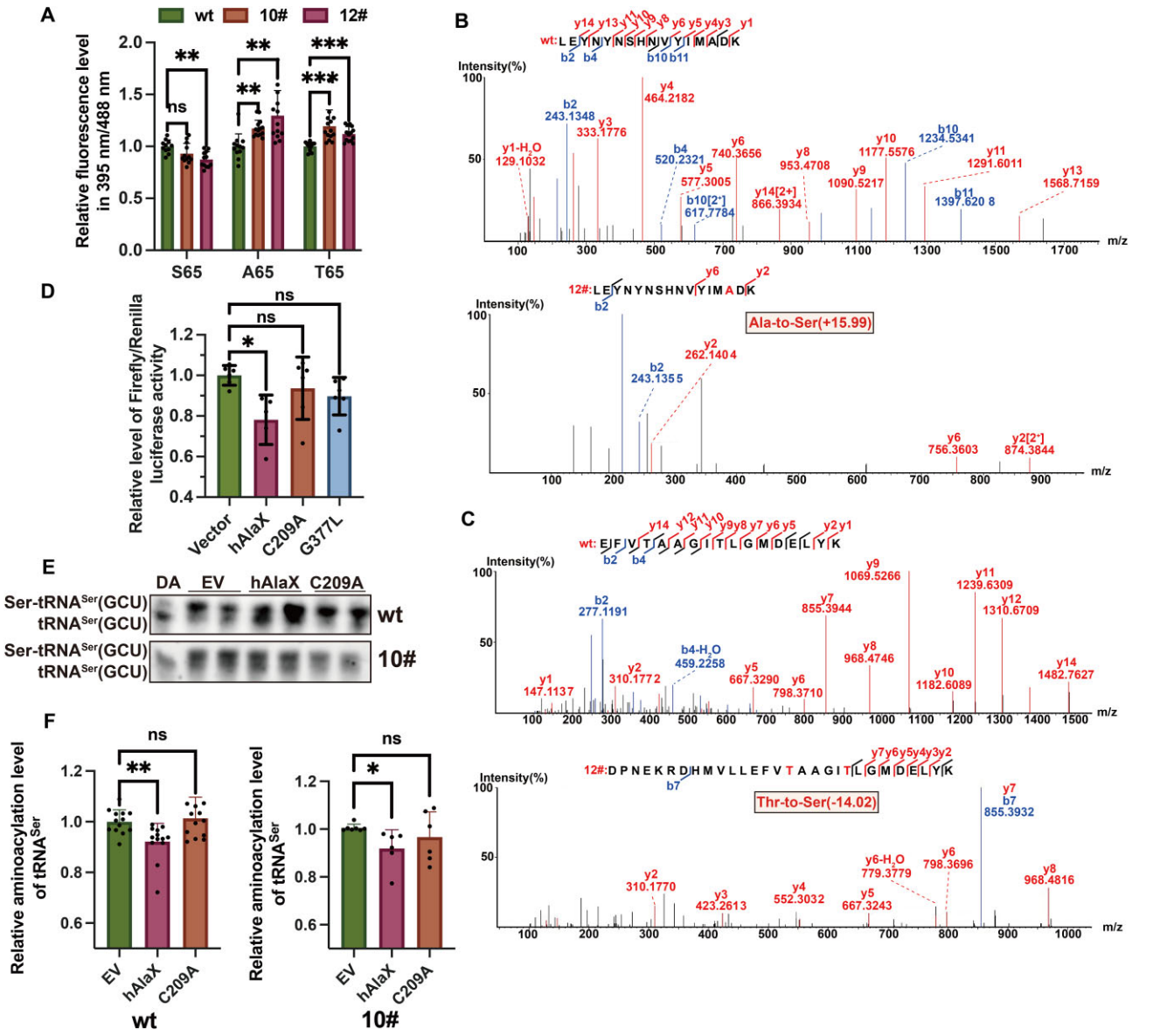

Figure 6. hAlaX is an active *trans*-editing factor in human cells. (**A**) Relative fluorescence level of overexpressed EGFP (T65) and its S65 and A65 mutants in 395 nm/488 nm in wild-type (wt) HEK293T and two KO cell lines (10# and 12#). (**B**) LC–MS/MS analysis of enriched EGFP from wild-type (upper, wt) and KO 12# (lower, 12#) cell lines. One Ala-to-Ser misincorporation occurrence is indicated by the red A. (**C**) LC–MS/MS analysis of enriched EGFP from wild-type (upper, wt) and KO 12# (lower, 12#) cell lines. Two Thr-to-Ser misincorporation occurrences are indicated by the red T. (**D**) Overexpression of wild-type hAlaX but not editing-deficient C209A and G377L suppressed decoding of consecutive Ser codons. The empty vector pCMV-3Tag-3A was introduced as the negative control. (**E**) A representative northern blotting gel to determine tRNA^{Ser}(GCU) charging level after wild-type hAlaX or C209A overexpression in HEK293T and KO 10# cells. The empty vector pCMV-3Tag-3A (EV) was introduced as the negative control. DA, deacylated sample. (**F**) Quantification of tRNA^{Ser}(GCU) charging level in (E). Data represent mean ± SD ($n = 12$ in (A), $n = 6$ in (D), $n = 13$ (wt) and $n = 6$–7 (KO 10#) in (F)). ns, no significance; *, $P < 0.05$; **, $P < 0.01$; ***, $P < 0.001$; mixed-effects analysis was performed in (A) and (D). Ordinary one-way analysis of variation was performed in (F).

corresponding EGFP fragment from wild-type cells did not contain any amino acid replacement (Supplementary Figure S17). Notably, the T65-harboring peptide was consistently not captured in the LC–MS/MS analyses of all purified EGFP samples, suggesting that proteolysis near this location is not favourable. Taken together, the results of direct peptide sequencing showed that the loss of hAlaX triggered misincorporation of Ser at the Ala and Thr codons in KO cells, suggesting that hAlaX acts as a guardian of translation quality by hydrolyzing Ser-tRNA^{Ala} and Ser-tRNA^{Thr} in mammalian cells.

The incorrect incorporation of amino acids into proteins interferes with their correct folding. Considering the higher level of Ser misincorporation in EGFP in KO cells, we co-expressed EGFP-FLAG with a hemagglutinin-tagged Ubiquitin in wild-type HEK293T cells and the two KO cell lines (10# & 12#). After the enrichment of EGFP-FLAG, western blotting showed that EGFP-FLAG from the two hAlaX KO cell lines was more ubiquitinated than that in wild-type cells (Supplementary Figure S18A).

We further monitored cell viability via hemocytometer counting and found that cell viability was comparable among

the three cell lines under physiological conditions; however, the addition of either 10 or 40 mM Ser to the cell culture significantly suppressed the growth of the two hAlaX KO cell lines, but not wild-type cells (Supplementary Figure S18B). In contrast, the addition of either Thr or Ala had no significant impact on the viability of each cell line (Supplementary Figures S18C, D), suggesting that the loss of Ser-mischarged tRNAs editing makes the cells more sensitive to Ser toxicity.

Overall, these results show that hAlaX can *trans*-edit Ser-tRNA^{Ala} and Ser-tRNA^{Thr} in mammalian cells, and the loss of this activity results in the incorporation of Ser at the Ala and Thr codons.

Overexpressed hAlaX hydrolyzes a trace fraction of Ser-tRNA^{Ser} in mammalian cells

Subsequently, we focused on the hydrolysis of Ser-tRNA^{Ser} by hAlaX in cells. Acid northern blotting analysis showed no significant change in Ser-tRNA^{Ser}(GCU) charging levels between wild-type HEK293T and two KO cell lines (Supplementary Figure S15D, E). We hypothesized that, under physiological conditions, capture and hydrolysis of Ser-tRNA^{Ser} (if it occurs) may represent only a very minor fraction of the charged tRNA^{Ser}, due to the efficient binding and protection of cognate aminoacyl-tRNAs by elongation factors for delivery to ribosomes (60). Based on this hypothesis, we overexpressed either wild-type hAlaX or the editing-deficient hAlaX-C209A mutant in wild-type HEK293T or KO 10# cells and then treated the cells with 1 μg/ml puromycin to interfere with protein synthesis flux, aiming to slow down the decoding speed and increase the accessibility of hAlaX to Ser-tRNA^{Ser}. We found that overexpression of wild-type hAlaX, but not hAlaX-C209A, slightly but significantly decreased the charging level of tRNA^{Ser}(GCU) (Figures 6E, F).

Moreover, we overexpressed and enriched hAlaX-FLAG by IP in HEK293T cells and performed northern blotting to determine whether tRNA^{Ser} was bound to hAlaX-FLAG. Both tRNA^{Ser}(GCU) and tRNA^{Ser}(AGA) were bound to hAlaX-FLAG; however, tRNA^{Lys}(UUU) was absent from the hAlaX-FLAG precipitate (Supplementary Figure S19A). Furthermore, we constructed a dual-luciferase reporter system, wherein six consecutive Ser codons (6 × AGC, decoded by tRNA^{Ser}(GCU)) were inserted upstream of the coding region of firefly luciferase, whereas the co-introduced coding region of renilla luciferase was not modified to serve as an expression control. We reasoned that if hAlaX was able to hydrolyze tRNA^{Ser}(GCU) in cells, the decreased amount of Ser-tRNA^{Ser}(GCU) after hAlaX-FLAG overexpression would potentially slow down the consecutive decoding of 6 × AGC codons due to a cumulative effect (Supplementary Figure S19B). We cotransfected HEK293T cells with a dual-luciferase reporter system and either an empty vector or a construct expressing hAlaX-FLAG. The overexpression of hAlaX-FLAG significantly reduced the amount of firefly luciferase (Supplementary Figure S19C). To verify the codon specificity of our dual-luciferase assay, we introduced consecutive Lys codons (6 × AAA, decoded by tRNA^{Lys}(UUU)) upstream of the firefly luciferase. As expected, the translation of the 6 × AAA-containing firefly luciferase was not affected by hAlaX overexpression (Supplementary Figure S19C). Finally, to ensure that the inhibitory effect on the decoding of consecutive Ser codon decoding derives from the editing function of hAlaX, two inactive mutants hAlaX-C209A and hAlaX-G377L were overexpressed under similar transfection conditions. As expected, both mutants failed to suppress the decoding efficiency of consecutive Ser codons (Figure 6D). The lack of decrease in firefly luciferase containing 6 × AGC upon overexpression of the hAlaX-C209A mutant suggests that hydrolysis of the Ser-tRNA^{Ser}, rather than tRNA^{Ser} sequestration, led to suppression of decoding, as the C209A mutation is unlikely to alter tRNA binding due to its deep localization in the editing pocket.

Altogether, these results suggest that overexpressed hAlaX can edit a trace amount of Ser-tRNA^{Ser} in mammalian cells, at least in some specific conditions.

Discussion

hAlaX is exclusively distributed in the cytoplasm but not in the mitochondria, suggesting that hAlaX only safeguards translation fidelity of cytoplasmic translation. Consistently, Mitoprot (61) predicted that hAlaX and *Sc*AlaX are cytoplasmic proteins. In addition, mitochondrial proteome profiling by several groups failed to identify AlaX (62,63). The above analyses suggest that editing by mitochondrial aaRSs is sufficient to prevent mistranslation under physiological conditions, possibly due to the relatively simple composition or lower concentrations of the mitochondrial amino acid pool (64). Without this layer of protection, disruption of the editing function of mitochondrial AlaRS and ThrRS leads to early embryonic lethality and cardiomyopathy (10–12).

Our data provide evidence that AlaXs from both lower and higher eukaryotes possess robust editing activities. A previous study reported the lack of editing activity of *Sc*AlaX for several (mis)charged tRNAs (27). One possible reason for the lack of editing activity by *Sc*AlaX could be that *Methanocaldococcus jannaschii* tRNA was used for the preparation of Ser-tRNA^{Thr} and Ser-tRNA^{Ala}, which might be poor substrates for *Sc*AlaX (27). It is also possible that the reaction mixture contains unknown elements that inactivate *Sc*AlaX. The activity of eukaryotic AlaXs demonstrates that an evolutionarily conserved *trans*-editing factor is constantly maintained for quality control of protein synthesis in all domains of life, although there are divergences in domain composition and sequence length.

In addition to editing Ser-tRNA^{Ala}, we found that both hAlaX and *Sc*AlaX actively hydrolyzed Ser-tRNA^{Thr}, a ThrRS substrate. LC–MS/MS results clearly showed that loss of *Sc*AlaX and hAlaX leads to Ala/Thr-to-Ser misincorporation, demonstrating that clearance of Ser-tRNA^{Ala} and Ser-tRNA^{Thr} occurs *in vivo* and that eukaryotic AlaXs serve as proofreaders for both AlaRS and ThrRS. Notably, the hydrolysis of Ser-tRNA^{Ala} by both bacterial AlaRS and archaeal AlaX is critically reliant on G3-U70 (17), and the transplantation of a single G3-U70 base pair in Ser-tRNA^{Thr} confers *M. mazeii* AlaX and *E. coli* AlaRS (438–875) editing activity toward Ser-tRNA^{Thr} (17). Ser-tRNA^{Thr}, Ser-tRNA^{Ser}, and Ser-tRNA^{Sec} hydrolysis by eukaryotic AlaXs clearly showed that editing by eukaryotic AlaXs was no longer dependent on G3-U70. Thus, the editing capability of eukaryotic AlaX as a ThrRS proofreader is likely due to its non-dependence on G30-U70 for tRNA recognition. A previous study showed that *Ph*AlaX-S was able to edit Ser-tRNA^{Thr} in addition to Ser-tRNA^{Ala}. The presence of a conserved Glu residue (E145) in *Ph*AlaX-S explains the extended tRNA specificity (26). Indeed, the corresponding residue R693 in *Ec*AlaRS was suggested to contact G3-U70 of tRNA^{Ala}. *Ec*AlaRS-R693K mutant was ready to

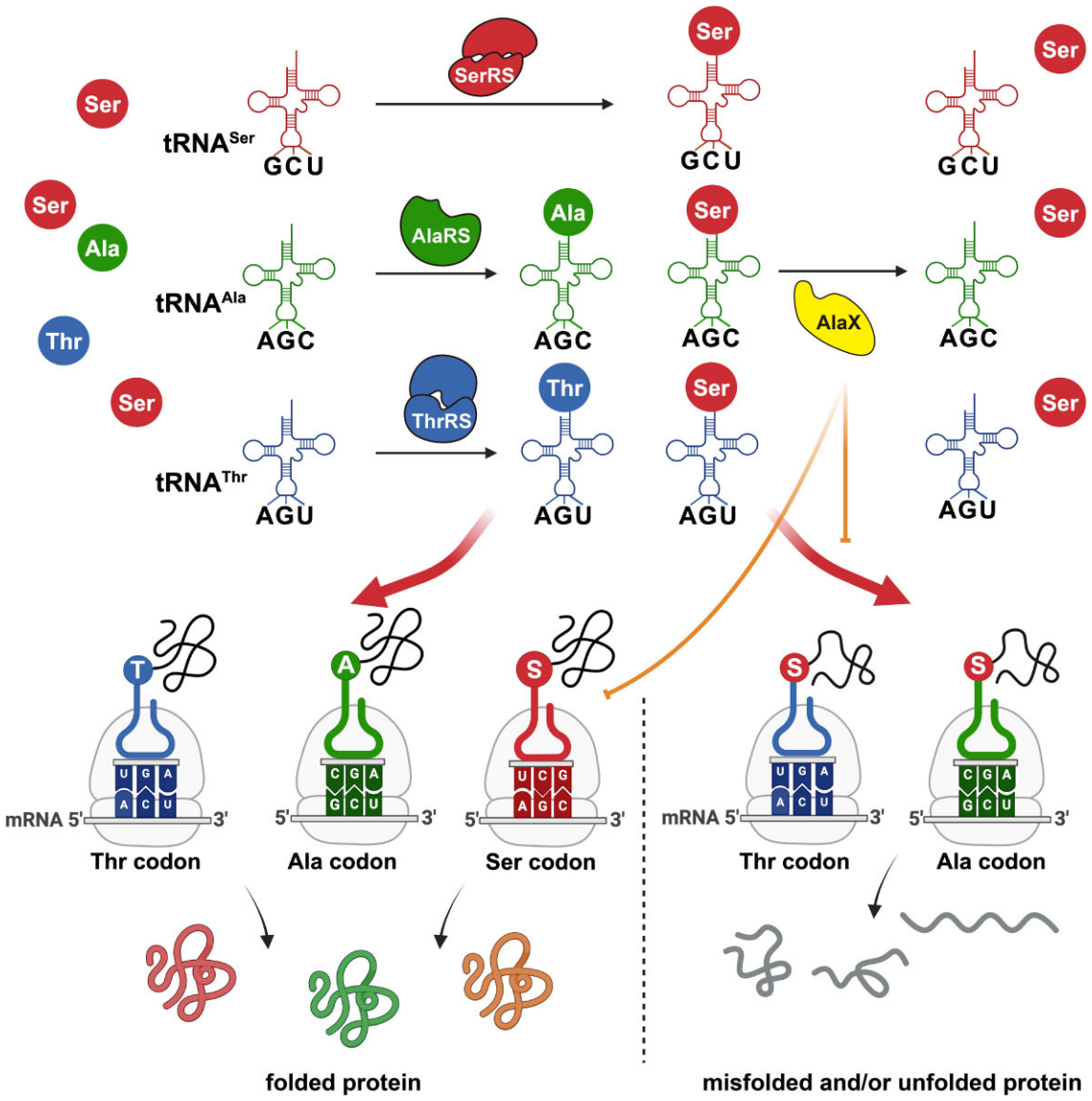

Figure 7. A proposed model showing AlaX being a tRNA-charging regulatory hub as a proofreader for AlaRS, ThrRS, and SerRS. Cytoplasmic AlaRS and ThrRS generate Ser-mischarged $tRNA^{Ala}$ and $tRNA^{Thr}$, a fraction that escapes *cis*-editing of AlaRS and ThrRS. The editing domain of AlaX was homologous to the ED domains of AlaRS and ThrRS. Eukaryotic AlaX can proofread Ser-$tRNA^{Ala}$ and Ser-$tRNA^{Thr}$ to prevent Ala-to-Ser and Thr-to-Ser translational errors, respectively, thereby limiting the generation of misfolded or unfolded proteins. Meanwhile, eukaryotic AlaX is capable of fine-tuning the abundance of Ser-$tRNA^{Ser}$ with a potential regulatory role in controlling the decoding speed of Ser codons. This figure was created with BioRender.com.

hydrolyze Ser-$tRNA^{Thr}$ (17). A hydrophobic residue (L270 or I239) was present at the corresponding position in *Sc*AlaX or hAlaX, likely explaining a broad tRNA specificity of eukaryotic AlaXs due to the lack of interaction between this residue and G3-U70.

The editing of Ser-$tRNA^{Ser}$ by eukaryotic AlaXs is unexpected but reasonable, given that recognition is independent of tRNA sequence. According to the tRNA channel theory, correctly charged tRNAs are immediately transferred to the elongation factor and ribosome (60). Thus, hAlaX appears to have little opportunity to capture Ser-$tRNA^{Ser}$. However, by IP and northern blotting, we verified that hAlaX does bind $tRNA^{Ser}$*in vivo*. Furthermore, the overexpression of active, but not catalytically inactive, hAlaX significantly impaired the translation of consecutive Ser codons. In addition, with translation blocked (puromycin treatment), hydrolysis of Ser-$tRNA^{Ser}$ by hAlaX was more pronounced. Finally, two independent reports using the DM-tRNA-seq (demethylase-thermostable group II intron RT tRNA sequencing) method showed that the aminoacylation levels of $tRNA^{Ser}$ isoacceptors are the lowest among all human tRNAs (65,66). The rationale for the low levels of Ser-$tRNA^{Ser}$ compared with other tRNAs (65,66) is unclear. Whether hydrolysis of Ser-$tRNA^{Ser}$ by hAlaX is responsible for the low $tRNA^{Ser}$ charging levels *in vivo* requires further investigation.

$mtRNA^{Ser}$(AGY) is the most unique tRNA in human cells since it lacks the entire D-arm. However, the minihelix comprising the amino acid acceptor and the T-arm exhibits a folding similar to that of the canonical tRNAs (47). The ability of hydrolysis of Ser-$mtRNA^{Ser}$(AGY) suggests recognition of the TφC-arm by C-Ala. However, deletion of the TψC-loop in $tRNA^{Ser}$ has less influence on Ser-$tRNA^{Ser}$ hydrolysis. There-

fore, understanding the interaction between C-Ala of hAlaX and the tRNA elbow region remains elusive. $tRNA^{Sec}$ is another unique tRNA, possessing a 9 + 4 minihelix structure (48). Compared with canonical tRNAs with a 7 + 5 minihelix, the distance between the elbow region (bound by the Gly-rich motif in C-Ala) and the CCA terminus (embedded in the active site of hAlaX) should be longer. Thus, we propose that hAlaX adopts a distinct conformation by extending the long helices between ED and C-Ala to accommodate $tRNA^{Sec}$. However, whether Ser-$tRNA^{Sec}$ is accessible for hAlaX editing *in vivo*, and if so, the significance of such editing requires further investigation. A recent study showed that Ser-$tRNA^{Sec}$ can escape the Sec synthesis pathway, suggesting the possibility of capturing Ser-$tRNA^{Sec}$ by hAlaX (67).

We observed little difference in the charging levels of $tRNA^{Ala}$, $tRNA^{Ser}$, and $tRNA^{Thr}$ in wild-type and hAlaX KO cells using acidic northern blotting. According to the discriminator factor of specific aaRSs, the catalytic efficiency for non-cognate amino acids is generally 2–3 orders of magnitude lower than that of cognate amino acids (29,30,32). In addition, the second sieve with AlaRS or ThrRS should remove *in situ* the majority of Ser-$tRNA^{Ala}$ or Ser-$tRNA^{Thr}$ (2). Thus, escaped Ser-mischarged $tRNA^{Ala}$ or $tRNA^{Thr}$ could represent less than 0.1–1% (deduced from the discriminator factor) of the $tRNA^{Ala}$ or $tRNA^{Thr}$ pool. Thus, it is reasonable to assume that the loss of hAlaX activity does not result in any observable accumulation of charged $tRNA^{Ala}$ or $tRNA^{Thr}$ in acidic northern blot. In addition, we propose that Ser-$tRNA^{Ser}$ hydrolysis may be minimal under physiological conditions due to a smooth translation cycle, leading to an insignificant difference between wild-type and hAlaX KO cells. Under specific conditions, like puromycin treatment in this study, Ser-$tRNA^{Ser}$ hydrolysis by hAlaX may be more pronounced.

Our results unexpectedly revealed completely different growth phenotypes in the presence of various translation inhibitors targeting distinct stages of protein synthesis in the ribosome (56,57). Loss of *Sc*AlaX made yeasts more sensitive to CHX, suggesting that accumulation of Ser-mischarged tRNAs is harmful to peptide elongation; however, it induced an obvious growth gain in the presence of G418 antibiotics, which was eliminated by overexpressing editing-capable AlaRS or ThrRS, suggesting that Ala-to-Ser or Thr-to-Ser mistranslation is beneficial under these stressful conditions. Considering that resistance to G418 or sensitivity to CHX was eliminated by overexpressing editing-capable but not editing-deficient AlaRS or ThrRS, we suggest that these effects were derived from mistranslation at Ala or Thr codons but not from regulation of Ser codon decoding. Tolerance to antibiotics or other stress treatments with mistranslation has been reported (68–70). Regardless of the detailed molecular mechanism, the gain of G418 resistance in yeasts with Ser mistranslation at the Ala or Thr codons expands the strategy employed by microorganisms to combat stressful growth environments.

In summary (Figure 7), we elucidate that eukaryotic AlaX is an active *trans*-editing factor *in vitro* and *in vivo*, with a strict Ser but a relaxed tRNA specificity. It functions as a freestanding factor to prevent the accumulation of both Ser-$tRNA^{Ala}$ and Ser-$tRNA^{Thr}$, escaping the *cis*-editing of AlaRS and ThrRS, respectively. The third checkpoint layer safeguards against mistranslation and maintains cellular homeostasis by limiting the generation of a statistical proteome in eukaryotes. Additionally, it exhibits the potential to fine-tune the Ser-$tRNA^{Ser}$ level, possibly to control mRNA translation efficiency under specific conditions with an unknown rationale. Our results uncover AlaX as a multiple-layer proofreader for AlaRS, ThrRS and SerRS and substantially enrich our knowledge of the mechanism of eukaryotic gene expression.

Data availability

All data presented in this study are available within the Figures, Table and in the Supplementary File.

Supplementary data

Supplementary Data are available at NAR Online.

Acknowledgements

We thank Drs Yi-Lin Li and Yue Yin in National Center for Protein Science Shanghai for LC–MS/MS analysis of amino acid misincorporation. We are grateful to Xue-Ling Mao, Meng-Han Huang, Jing-Bo Zhou and Gui-Xin Peng in Zhou lab for technical assistance. We also thank Dr Gilbert Eriani (University of Strasbourg) for carefully reading the manuscript. Graphic abstract was created with BioRender.com.

Author contributions: X.L.Z. conceived the study, designed the experiments, analyzed the data, drafted and revised the manuscript. Z.H.L. performed experiments, analyzed data and drafted the manuscript.

Funding

Strategic Priority Research Program of the Chinese Academy of Sciences [XDB0570000]; National Key Research and Development Program of China [2021YFA1300800, 2021YFC2700903]; Natural Science Foundation of China [32271300]; Committee of Science and Technology in Shanghai [22ZR1481300, 22JC1400503]; CAS Project for Young Scientists in Basic Research [YSBR-075]. Funding for open access charge: Research grant.

Conflict of interest statement

None declared.

References

1. Ibba,M. and Söll,A.D. (1999) Quality control mechanisms during translation. *Science*, **286**, 1893–1897.
2. Ling,J., Reynolds,N. and Ibba,M. (2009) Aminoacyl-tRNA synthesis and translational quality control. *Annu. Rev. Microbiol.*, **63**, 61–78.
3. Ibba,M. and Söll,D. (2000) Aminoacyl-tRNA synthesis. *Annu. Rev. Biochem.*, **69**, 617–650.
4. Guo,M., Yang,X.-L. and Schimmel,P. (2010) New functions of aminoacyl-tRNA synthetases beyond translation. *Nat. Rev. Mol. Cell Biol.*, **11**, 668–674.
5. Schmidt,E. and Schimmel,P. (1994) Mutational isolation of a sieve for editing in a transfer-Rna synthetase. *Science*, **264**, 265–267.
6. Zhou,X. and Wang,E. (2013) Transfer RNA: a dancer between charging and mis-charging for protein biosynthesis. *Sci. China Life Sci.*, **56**, 921–932.
7. Lin,L., Hale,S.P. and Schimmel,P. (1996) Aminoacylation error correction. *Nature*, **384**, 33–34.

8. Chen,J.-F., Guo,N.-N., Li,T., Wang,E.-D. and Wang,Y.-L. (2000) CP1 domain in leucyl-tRNA synthetase is crucial for its editing function. *Biochemistry*, **39**, 6726–6731.
9. Nangle,L.A., Motta,C.M. and Schimmel,P. (2006) Global effects of mistranslation from an editing defect in mammalian cells. *Chem. Biol.*, **13**, 1091–1100.
10. Lee,J.W., Beebe,K., Nangle,L.A., Jang,J., Longo-Guess,C.M., Cook,S.A., Davisson,M.T., Sundberg,J.P., Schimmel,P. and Ackerman,S.L. (2006) Editing-defective tRNA synthetase causes protein misfolding and neurodegeneration. *Nature*, **443**, 50–55.
11. Liu,Ye, Satz,J.S., Vo,My-N, Nangle,L.A., Schimmel,P. and Ackerman,S.L. (2014) Deficiencies in tRNA synthetase editing activity cause cardioproteinopathy. *Proc. Natl. Acad. Sci. U.S.A.*, **111**, 17570–17575.
12. Zheng,W.-Q., Zhang,J.-H., Li,Zi-H, Liu,X., Zhang,Y., Huang,S., Li,J., Zhou,B., Eriani,G., Wang,E.-D., *et al.* (2023) Mammalian mitochondrial translation infidelity leads to oxidative stress-induced cell cycle arrest and cardiomyopathy. *Proc. Natl. Acad. Sci. U.S.A.*, **120**, e2309714120.
13. Liu,Z., Vargas-Rodriguez,O., Goto,Y., Novoa,E.M., Ribas De Pouplana,L., Suga,H. and Musier-Forsyth,K. (2015) Homologous *trans*-editing factors with broad tRNA specificity prevent mistranslation caused by serine/threonine misactivation. *Proc. Natl. Acad. Sci. U.S.A.*, **112**, 6027–6032.
14. Pawar,K.I., Suma,K., Seenivasan,A., Kuncha,S.K., Routh,S.B., Kruparani,S.P. and Sankaranarayanan,R. (2017) Role of D-aminoacyl-tRNA deacylase beyond chiral proofreading as a cellular defense against glycine mischarging by AlaRS. *eLife*, **6**, e24001.
15. Hauth,F., Funck,D. and Hartig,J.S. (2023) A standalone editing protein deacylates mischarged canavanyl-tRNA^{Arg} to prevent canavanine incorporation into proteins. *Nucleic Acids Res.*, **51**, 2001–2010.
16. Kuzmishin Nagy,A.B., Bakhtina,M. and Musier-Forsyth,K. (2020) *Trans*-editing by aminoacyl-tRNA synthetase-like editing domains. *Enzymes*, **48**, 69–115.
17. Beebe,K., Mock,M., Merriman,E. and Schimmel,P. (2008) Distinct domains of tRNA synthetase recognize the same base pair. *Nature*, **451**, 90–93.
18. Naganuma,M., Sekine,S.-I., Chong,Y.E., Guo,M., Yang,X.-L., Gamper,H., Hou,Y.-M, Schimmel,P. and Yokoyama,S. (2014) The selective tRNA aminoacylation mechanism based on a single G•U pair. *Nature*, **510**, 507–511.
19. Guo,M., Chong,Y.E., Shapiro,R., Beebe,K., Yang,X.-L. and Schimmel,P. (2009) Paradox of mistranslation of serine for alanine caused by AlaRS recognition dilemma. *Nature*, **462**, 808–812.
20. An,S. and Musier-Forsyth,K. (2004) *Trans*-editing of cys-tRNA^{Pro} by Haemophilus influenzae YbaK protein. *J. Biol. Chem.*, **279**, 42359–42362.
21. Ruan,B. and Söll,D. (2005) The bacterial YbaK protein is a cys-tRNA and cys-tRNA deacylase. *J. Biol. Chem.*, **280**, 25887–25891.
22. Korencic,D., Ahel,I., Schelert,J., Sacher,M., Ruan,B., Stathopoulos,C., Blum,P., Ibba,M. and Söll,D. (2004) A freestanding proofreading domain is required for protein synthesis quality control in Archaea. *Proc. Natl. Acad. Sci. U.S.A.*, **101**, 10260–10265.
23. Sokabe,M., Okada,A., Yao,M., Nakashima,T. and Tanaka,I. (2005) Molecular basis of alanine discrimination in editing site. *Proc. Natl. Acad. Sci. U.S.A.*, **102**, 11669–11674.
24. Fukunaga,R. and Yokoyama,S. (2007) Structure of the AlaX-M *trans*-editing enzyme from *Pyrococcus horikoshii*. *Acta Crystallogr. D*, **63**, 390–400.
25. Chong,Y.E., Yang,X.-L. and Schimmel,P. (2008) Natural homolog of tRNA synthetase editing domain rescues conditional lethality caused by mistranslation. *J. Biol. Chem.*, **283**, 30073–30078.
26. Novoa,E.M., Vargas-Rodriguez,O., Lange,S., Goto,Y., Suga,H., Musier-Forsyth,K. and Ribas De Pouplana,L. (2015) Ancestral AlaX editing enzymes for control of genetic code fidelity are not tRNA-specific. *J. Biol. Chem.*, **290**, 10495–10503.
27. Ahel,I., Korencic,D., Ibba,M. and Söll,D. (2003) *Trans*-editing of mischarged tRNAs. *Proc. Natl. Acad. Sci. U.S.A.*, **100**, 15422–15427.
28. Nawaz,M.H., Merriman,E. and Yang,X.L., and Schimmel P. (2011) p23H implicated as cis/trans regulator of AlaXp-directed editing for mammalian cell homeostasis. *Proc. Natl. Acad. Sci. U.S.A.*, **108**, 2723–2728.
29. Zhou,X.-L., Ruan,Z.-R., Huang,Q., Tan,M. and Wang,E.-D (2013) Translational fidelity maintenance preventing ser mis-incorporation at thr codon in protein from eukaryote. *Nucleic Acids Res.*, **41**, 302–314.
30. Zeng,Qi-Yu, Peng,G.-X., Li,G., Zhou,J.-B., Zheng,W.-Q., Xue,M.-Q., Wang,E.-D and Zhou,X.-L. (2019) The G3-U70-independent tRNA recognition by human mitochondrial alanyl-tRNA synthetase. *Nucleic Acids Res.*, **47**, 3072–3085.
31. Mao,X.-L., Li,Z.-H, Huang,M.-H., Wang,J.-T., Zhou,J.-B., Li,Q.-R., Xu,H., Wang,Xi-J and Zhou,X.-L. (2021) Mutually exclusive substrate selection strategy by human m^{3}C RNA transferases METTL2A and METTL6. *Nucleic Acids Res.*, **49**, 8309–8323.
32. Chen,Y., Ruan,Z.-R., Wang,Y., Huang,Q., Xue,M.-Q., Zhou,X.-L. and Wang,E.-D. (2018) A threonyl-tRNA synthetase-like protein has tRNA aminoacylation and editing activities. *Nucleic Acids Res.*, **46**, 3643–3656.
33. Zhou,X.-L., Zhu,B. and Wang,E.-D. (2008) The CP2 domain of leucyl-tRNA synthetase is crucial for amino acid activation and post-transfer editing. *J. Biol. Chem.*, **283**, 36608–36616.
34. Zhou,J.-B., Wang,Y., Zeng,Q.-Y., Meng,S.-X., Wang,E.-D. and Zhou,X.-L. (2020) Molecular basis for t^{6}A modification in human mitochondria. *Nucleic Acids Res.*, **48**, 3181–3194.
35. Huang,M.-H., Wang,J.-T., Zhang,J.-H., Mao,X.-L., Peng,G.-X., Lin,X., Lv,D., Yuan,C., Lin,H., Wang,En-D, *et al.* (2023) Mitochondrial RNA m^{3}C methyltransferase METTL8 relies on an isoform-specific N-terminal extension and modifies multiple heterogenous tRNAs. *Sci. Bull.*, **68**, 2094–2105.
36. Zhou,X.-L., Fang,Z.-P., Ruan,Z.-R., Wang,M., Liu,Ru-J, Tan,M., Anella,F.M. and Wang,En-D (2013) Aminoacylation and translational quality control strategy employed by leucyl-tRNA synthetase from a human pathogen with genetic code ambiguity. *Nucleic Acids Res.*, **41**, 9825–9838.
37. Peng,G.-X., Mao,X.-L., Cao,Y., Yao,S.-Y., Li,Q.-R., Chen,X., Wang,E.-D. and Zhou,X.-L. (2022) RNA granule-clustered mitochondrial aminoacyl-tRNA synthetases form multiple complexes with the potential to fine-tune tRNA aminoacylation. *Nucleic Acids Res.*, **50**, 12951–12968.
38. Zhou,X.-L., Chen,Y., Zeng,Qi-Yu, Ruan,Z.-R., Fang,P. and Wang,E.-D. (2019) Newly acquired N-terminal extension targets threonyl-tRNA synthetase-like protein into the multiple tRNA synthetase complex. *Nucleic Acids Res.*, **47**, 8662–8674.
39. Peng,G.-X., Zhang,Y., Wang,Q.-Q., Li,Q.-R., Xu,H., Wang,E.-D. and Zhou,X.-L. (2021) The human tRNA taurine modification enzyme GTPBP3 is an active GTPase linked to mitochondrial diseases. *Nucleic Acids Res.*, **49**, 2816–2834.
40. Jumper,J., Evans,R., Pritzel,A., Green,T., Figurnov,M., Ronneberger,O., Tunyasuvunakool,K., Bates,R., Žídek,A., Potapenko,A., *et al.* (2021) Highly accurate protein structure prediction with AlphaFold. *Nature*, **596**, 583–589.
41. Varadi,M., Anyango,S., Deshpande,M., Nair,S., Natassia,C., Yordanova,G., Yuan,D., Stroe,O., Wood,G., Laydon,A., *et al.* (2022) AlphaFold Protein Structure Database: massively expanding the structural coverage of protein-sequence space with high-accuracy models. *Nucleic Acids Res.*, **50**, D439–D444.
42. Sun,L., Wei,N., Kuhle,B., Blocquel,D., Novick,S., Matuszek,Z., Zhou,H., He,W., Zhang,J., Weber,T., *et al.* (2021) CMT2N-causing aminoacylation domain mutants enable Nrp1 interaction with AlaRS. *Proc. Natl. Acad. Sci. U.S.A.*, **118**, e2012898118.

43. Naganuma,M., Sekine,S.-I., Fukunaga,R. and Yokoyama,S. (2009) Unique protein architecture of alanyl-tRNA synthetase for aminoacylation, editing, and dimerization. *Proc. Natl. Acad. Sci. U.S.A.*, **106**, 8489–8494.
44. Beebe,K., De Pouplana,L.R. and Schimmel,P. (2003) Elucidation of tRNA-dependent editing by a class II tRNA synthetase and significance for cell viability. *EMBO J.*, **22**, 668–675.
45. Wang,Y., Zhou,X.-L., Ruan,Z.-R., Liu,Ru-J, Eriani,G. and Wang,E.-D. (2016) A Human disease-causing point mutation in mitochondrial threonyl-tRNA synthetase induces both structural and functional defects. *J. Biol. Chem.*, **291**, 6507–6520.
46. Yu,T., Zhang,Yi, Zheng,W.-Q., Wu,S., Li,G., Zhang,Y., Li,N., Yao,R., Fang,P., Wang,J., *et al.* (2022) Selective degradation of $tRNA^{Ser}$(AGY) is the primary driver for mitochondrial seryl-tRNA synthetase-related disease. *Nucleic Acids Res.*, **50**, 11755–11774.
47. Kuhle,B., Hirschi,M., Doerfel,L.K., Lander,G.C. and Schimmel,P. (2022) Structural basis for shape-selective recognition and aminoacylation of a D-armless human mitochondrial tRNA. *Nat. Commun.*, **13**, 5100.
48. Palioura,S., Sherrer,R.L., Steitz,T.A., Söll,D. and Simonović,M. (2009) The human SepSecS-tRNA complex reveals the mechanism of selenocysteine formation. *Science*, **325**, 321–325.
49. Giegé,R. and Eriani,G. (2023) The tRNA identity landscape for aminoacylation and beyond. *Nucleic Acids Res.*, **51**, 1528–1570.
50. Suzuki,T., Nagao,A. and Suzuki,T. (2011) Human mitochondrial tRNAs: biogenesis, function, structural aspects, and diseases. *Annu. Rev. Genet.*, **45**, 299–329.
51. Dock-Bregeon,A.-C., Sankaranarayanan,R., Romby,P., Caillet,J., Springer,M., Rees,B., Francklyn,C.S., Ehresmann,C. and Moras,D. (2000) Transfer RNA-mediated editing in threonyl-tRNA synthetase. The class II solution to the double discrimination problem. *Cell*, **103**, 877–884.
52. Hilander,T., Zhou,X.-L., Konovalova,S., Zhang,Fu-P, Euro,L., Chilov,D., Poutanen,M., Chihade,J., Wang,En-D and Tyynismaa,H. (2018) Editing activity for eliminating mischarged tRNAs is essential in mammalian mitochondria. *Nucleic Acids Res.*, **46**, 849–860.
53. Zhang,H., Wu,J., Lyu,Z. and Ling,J. (2021) Impact of alanyl-tRNA synthetase editing deficiency in yeast. *Nucleic Acids Res.*, **49**, 9953–9964.
54. Sun,L., Song,Y., Blocquel,D., Yang,X.-L. and Schimmel,P. (2016) Two crystal structures reveal design for repurposing the C-Ala domain of human AlaRS. *Proc. Natl. Acad. Sci. U.S.A.*, **113**, 14300–14305.
55. Kuhle,B., Chihade,J. and Schimmel,P. (2020) Relaxed sequence constraints favor mutational freedom in idiosyncratic metazoan mitochondrial tRNAs. *Nat. Commun.*, **11**, 969.
56. Prokhorova,I., Altman,R.B., Djumagulov,M., Shrestha,J.P., Urzhumtsev,A., Ferguson,A., Chang,C.-W.T., Yusupov,M., Blanchard,S.C. and Yusupova,G. (2017) Aminoglycoside interactions and impacts on the eukaryotic ribosome. *Proc. Natl. Acad. Sci. U.S.A.*, **114**, E10899–E10908.
57. Schneider-Poetsch,T., Ju,J., Eyler,D.E., Dang,Y., Bhat,S., Merrick,W.C., Green,R., Shen,B. and Liu,J.O. (2010) Inhibition of eukaryotic translation elongation by cycloheximide and lactimidomycin. *Nat. Chem. Biol.*, **6**, 209–217.
58. Patterson,G.H., Knobel,S.M., Sharif,W.D., Kain,S.R. and Piston,D.W. (1997) Use of the green fluorescent protein and its mutants in quantitative fluorescence microscopy. *Biophys. J.*, **73**, 2782–2790.
59. Cormack,B.P., Valdivia,R.H. and Falkow,S. (1996) FACS-optimized mutants of the green fluorescent protein (GFP). *Gene*, **173**, 33–38.
60. Sivaram,P. and Deutscher,M.P. (1990) Existence of two forms of rat liver arginyl-tRNA synthetase suggests channeling of aminoacyl-tRNA for protein synthesis. *Proc. Natl. Acad. Sci. U.S.A.*, **87**, 3665–3669.
61. Claros,M.G. and Vincens,P. (1996) Computational method to predict mitochondrially imported proteins and their targeting sequences. *Eur. J. Biochem.*, **241**, 779–786.
62. Rath,S., Sharma,R., Gupta,R., Ast,T., Chan,C., Durham,T.J., Goodman,R.P., Grabarek,Z., Haas,M.E., Hung,W.H.W., *et al.* (2021) MitoCarta3.0: an updated mitochondrial proteome now with sub-organelle localization and pathway annotations. *Nucleic Acids. Res.*, **49**, D1541–D1547.
63. Morgenstern,M., Peikert,C.D., Lübbert,P., Suppanz,I., Klemm,C., Alka,O., Steiert,C., Naumenko,N., Schendzielorz,A., Melchionda,L., *et al.* (2021) Quantitative high-confidence human mitochondrial proteome and its dynamics in cellular context. *Cell Metab.*, **33**, 2464–2483.
64. Ross-Inta,C., Tsai,C.-Y. and Giulivi,C. (2008) The mitochondrial pool of free amino acids reflects the composition of mitochondrial DNA-encoded proteins: indication of a post-translational quality control for protein synthesis. *Biosci. Rep.*, **28**, 239–249.
65. Evans,M.E., Clark,W.C., Zheng,G. and Pan,T. (2017) Determination of tRNA aminoacylation levels by high-throughput sequencing. *Nucleic Acids Res.*, **45**, e133.
66. Davidsen,K. and Sullivan,L.B. (2024) A robust method for measuring aminoacylation through tRNA-Seq. bioRxiv doi: https://doi.org/10.1101/2023.07.31.551363, 06 March 2024, preprint: not peer reviewed.
67. Liu,Z., Wang,J., Shi,Y., Yee,B.A., Terrey,M., Zhang,Q., Lee,J.-C., Lin,K.-I., Wang,A.H.-J., Ackerman,S.L., *et al.* (2023) Seryl-tRNA synthetase promotes translational readthrough by mRNA binding and involvement of the selenocysteine incorporation machinery. *Nucleic Acids Res.*, **51**, 10768–10781.
68. Pezo,V., Metzgar,D., Hendrickson,T.L., Waas,W.F., Hazebrouck,S., Döring,V., Marlière,P., Schimmel,P. and De Crécy-Lagard,V. (2004) Artificially ambiguous genetic code confers growth yield advantage. *Proc. Natl. Acad. Sci. U.S.A.*, **101**, 8593–8597.
69. Javid,B., Sorrentino,F., Toosky,M., Zheng,W., Pinkham,J.T., Jain,N., Pan,M., Deighan,P. and Rubin,E.J. (2014) Mycobacterial mistranslation is necessary and sufficient for rifampicin phenotypic resistance. *Proc. Natl. Acad. Sci. U.S.A.*, **111**, 1132–1137.
70. Schuntermann,D.B., Fischer,J.T., Bile,J., Gaier,S.A., Shelley,B.A., Awawdeh,A., Jahn,M., Hoffman,K.S., Westhof,E., Söll,D., *et al.* (2023) Mistranslation of the genetic code by a new family of bacterial transfer RNAs. *J. Biol. Chem.*, **299**, 104852.

Received: January 30, 2024. **Editorial Decision:** May 21, 2024. **Accepted:** May 27, 2024